

1 **Interaction of CO<sub>2</sub> concentrations and water stress in**  
2 **semi-arid plants causes diverging response in instantaneous**  
3 **water use efficiency and carbon isotope composition**

4 Na Zhao<sup>1,3</sup>, Ping Meng<sup>2</sup>, Yabing He<sup>1</sup>, Xinxiao Yu<sup>1,3\*</sup>

5 <sup>1</sup> College of soil and water conservation, Beijing Forestry University, Beijing 100083, P.R. China

6 <sup>2</sup> Research Institute of Forestry, Chinese Academy of Forestry 100091, Beijing, P.R. China

7 <sup>3</sup> Beijing collaborative innovation center for eco-environmental improvement with forestry and  
8 fruit trees

9 **Abstract.** In the context of global warming attributable to the increasing levels of CO<sub>2</sub>, severe drought  
10 may be more frequent in areas with chronic water shortages (semi-arid areas). This necessitates  
11 research on the interactions between increased levels of CO<sub>2</sub> and drought on plant photosynthesis. It is  
12 commonly reported that <sup>13</sup>C fractionation occurs as CO<sub>2</sub>-gas diffuses from the atmosphere to the  
13 sub-stomatal cavity. Few researchers have investigated <sup>13</sup>C fractionation at the site of carboxylation to  
14 cytoplasm before sugars are exported outward from the leaf. This process typically progresses in  
15 response to variations in environmental conditions (i.e., CO<sub>2</sub> concentrations and water stress),  
16 including in their interaction. Therefore, saplings of two typical plant species (*Platycladus orientalis*  
17 and *Quercus variabilis*) from semi-arid areas of Northern China were selected and cultivated in growth  
18 chambers with orthogonal treatments (four CO<sub>2</sub> concentrations ([CO<sub>2</sub>]) × five soil volumetric water  
19 content (SWC)). The δ<sup>13</sup>C of water-soluble compounds extracted from leaves of saplings was  
20 determined for instantaneous water use efficiency (WUE<sub>cp</sub>) after cultivation. Instantaneous water use  
21 efficiency derived from gas exchange (WUE<sub>ge</sub>) was integrated to estimate differences in δ<sup>13</sup>C signal  
22 variation before leaf-level translocation of primary assimilates. The WUE<sub>ge</sub> of *P. orientalis* and *Q.*  
23 *variabilis* both decreased with increased soil moisture at 35%–80% of field capacity (FC), and  
24 increased with elevated [CO<sub>2</sub>] by increasing photosynthetic capacity and reducing transpiration.  
25 Instantaneous water use efficiency (iWUE) according to environmental changes, differed between the  
26 two species. The WUE<sub>ge</sub> in *P. orientalis* was significantly greater than that in *Q. variabilis*, while an  
27 opposite trend was observed when comparing WUE<sub>cp</sub> between the two species. Total <sup>13</sup>C fractionation  
28 at the site of carboxylation to cytoplasm before sugar export (total <sup>13</sup>C fractionation) was  
29 species-specific, as demonstrated in the interaction of [CO<sub>2</sub>] and SWC. Rising [CO<sub>2</sub>] coupled with  
30 moistened soil generated increasing disparities in δ<sup>13</sup>C between water-soluble compounds (δ<sup>13</sup>C<sub>WSC</sub>)  
31 and estimates based on gas-exchange observations (δ<sup>13</sup>C<sub>obs</sub>) in *P. orientalis*, ranging between  
32 0.0328‰–0.0472‰. Differences between δ<sup>13</sup>C<sub>WSC</sub> and δ<sup>13</sup>C<sub>obs</sub> in *Q. variabilis* increased as [CO<sub>2</sub>] and  
33 SWC increased (0.0384‰–0.0466‰). The <sup>13</sup>C fractionation from mesophyll conductance (g<sub>m</sub>) and  
34 post-carboxylation both contributed to the total <sup>13</sup>C fractionation that was determined by δ<sup>13</sup>C of  
35 water-soluble compounds and gas-exchange measurements. Total <sup>13</sup>C fractionation was linearly  
36 dependent on stomatal conductance, indicating post-carboxylation fractionation could be attributed to  
37 environmental variation. The magnitude and environmental dependence of apparent post-carboxylation  
38 fractionation is worth our attention when addressing photosynthetic fractionation.

x —  
Something is missing

an assessment of?

tendency

x —  
x —

39 **Key words:** Post-carboxylation fractionation; Carbon isotope fractionation; Elevated CO<sub>2</sub>  
40 concentration; Soil volumetric water content; Instantaneous water use efficiency

## 41 1 Introduction

42 Since the industrial revolution, atmospheric CO<sub>2</sub> concentration has increased at an annual rate of  
43 0.4%, and is expected to increase to 700 μmol·mol<sup>-1</sup>, culminating in more frequent periods of dryness  
44 (IPCC, 2014). Increasing atmospheric CO<sub>2</sub> concentrations that exacerbate the greenhouse effect will  
45 increase fluctuations in global precipitation patterns, <sup>which</sup> but will probably amplify drought frequency in  
46 arid regions, <sup>flooding</sup> and lead to more frequent extreme events in humid regions (Lobell et al., 2014). —X  
47 Accompanying the increasing concentration of CO<sub>2</sub>, mean δ<sup>13</sup>C of atmospheric CO<sub>2</sub> is currently being  
48 depleted by 0.02‰–0.03‰ year<sup>-1</sup> (CU-INSTAAR/NOAACMDL network for atmospheric CO<sub>2</sub>;  
49 <http://www.esrl.noaa.gov/gmd/>).

50 The current carbon isotopic composition may respond to environmental change and <sup>its</sup> their influence —X  
51 on diffusion via plant physiological and metabolic processes (Gessler et al., 2014; Streit et al., 2013).  
52 While depletion of δ<sup>13</sup>C<sub>CO<sub>2</sub></sub> is occurring in the atmosphere, variations in CO<sub>2</sub> concentration ([CO<sub>2</sub>])  
53 may affect δ<sup>13</sup>C of plant organs <sup>which</sup> that, in turn, ~~are~~ <sup>are</sup> responding physiologically to changes in climate —X  
54 (Gessler et al., 2014). The carbon discrimination (<sup>Δ</sup><sup>13</sup>A) of leaves could also provide timely feedback  
55 about the availability of soil moisture and ~~the~~ atmospheric vapor pressure deficit (Cernusak et al.,  
56 2012). Discrimination of <sup>13</sup>C in leaves relies mainly on environmental factors that affect the ratio of  
57 intercellular to ambient [CO<sub>2</sub>] (C<sub>i</sub>/C<sub>a</sub>). Rubisco activities and the mesophyll conductance derived from  
58 the difference of [CO<sub>2</sub>] between intercellular sites and chloroplasts are also involved (Farquhar et al.,  
59 1982; Cano et al., 2014). Changes in environmental conditions affect photosynthetic discrimination,  
60 ~~recording~~ differentially in the δ<sup>13</sup>C of water-soluble compounds (δ<sup>13</sup>C<sub>WSC</sub>) in different plant organs.  
61 Several processes during photosynthesis alter the δ<sup>13</sup>C of carbon transported within plants.  
62 Carbon-fractionation during photosynthetic CO<sub>2</sub> fixation has been reviewed elsewhere (Farquhar et al.,  
63 1982; Farquhar and Sharkey, 1982).

64 Post-photosynthetic fractionation is derived from equilibrium and kinetic isotopic effects that  
65 determine isotopic differences between metabolites and intramolecular reaction positions. These are  
66 defined as “post-photosynthetic” or “post-carboxylation” fractionation (Jäggi et al., 2002; Badeck et al.,  
67 2005; Gessler et al., 2008). Post-carboxylation fractionation in plants includes the carbon  
68 discrimination that follows carboxylation of ribulose-1, 5-bisphosphate, and internal diffusion (RuBP,  
69 27‰), as well as related transitory starch metabolism (Gessler et al., 2008; Gessler et al., 2014) <sup>more</sup>  
70 fractionation in leaves, fractionation-associated phloem transport, remobilization or storage of soluble  
71 carbohydrates, and starch metabolism fractionation in sink tissue (tree rings). In the synthesis of  
72 soluble sugars, <sup>13</sup>C-depletions of triose phosphates occur during ~~export~~ from the cytoplasm, and during  
73 production of fructose-1, 6-bisphosphate by aldolase in transitory starch synthesis (Rossmann  
74 et al., 1991; Gleixner and Schmidt, 1997). Synthesis of sugars before transportation to the twig is  
75 associated with the post-carboxylation fractionation generated in leaves. Although these are likely to  
76 play a role, another consideration is [CO<sub>2</sub>] in the chloroplast (C<sub>c</sub>), not in the intercellular space, as <sup>used</sup> <sup>considered</sup>  
77 in the simplified equation of Farquhar’s model (Evans et al., 1986; Farquhar et al., 1989) is actually  
78 defined as carbon isotope discrimination (δ<sup>13</sup>C). Differences between gas-exchange derived values and  
79 online measurements of δ<sup>13</sup>C have often been used to estimate C<sub>i</sub>-C<sub>c</sub> and mesophyll conductance for  
80 CO<sub>2</sub> (Le Roux et al., 2001; Warren and Adams, 2006; Flexas et al., 2006; Evans et al., 2009; Flexas et  
81 al., 2012; Evans and von Caemmerer 2013). In this regard, changes in mesophyll conductance could be

124 growth chambers (A and B) were used in this study. Chamber A maintained [CO<sub>2</sub>] at 400 ppm (C<sub>400</sub>)  
125 and 500 ppm (C<sub>500</sub>). Chamber B maintained [CO<sub>2</sub>] at 600 ppm (C<sub>600</sub>) and 800 ppm (C<sub>800</sub>). The target  
126 [CO<sub>2</sub>] in each chamber had a standard deviation of ± 50 ppm during plant cultivation and testing.

127 An automatic watering device was used to irrigate the potted saplings to avoid heterogeneity when  
128 scheduled watering was not made (Fig. 1). The watering device consisted of a water storage tank,  
129 holder, controller, soil moisture sensors, and drip irrigation component. Prior to use, the tank was filled  
130 with water, and the soil moisture sensor was inserted to a uniform depth in the soil. After connecting  
131 the controller to an AC power supply, target soil volumetric water content (SWC) could be set and  
132 monitored by soil moisture sensors. Since changes in SWC could be sensed by the sensors, this  
133 automatic watering device can be regulated to begin watering or stop watering the plants. One  
134 irrigation device was installed per chamber. Based on mean field capacity (FC) of potted soil (30.70%),  
135 we established orthogonal treatments of four [CO<sub>2</sub>] × five SWCs (Tab. 1). In Table 1, A<sub>1</sub>-A<sub>4</sub> denotes  
136 [CO<sub>2</sub>] of 400 ppm (C<sub>400</sub>), 500 ppm (C<sub>500</sub>), 600 ppm (C<sub>600</sub>) and 800 ppm (C<sub>800</sub>) in the chambers; B<sub>1</sub>-B<sub>5</sub>  
137 denotes 35%–45% of FC (10.74%–13.81%), 50%–60% of FC (15.35%–18.42%), 60%–70% of FC  
138 (18.42%–21.49%), and 70%–80% of FC (21.49%–24.56%) and 100% of FC (CK, 27.63%–30.70%).  
139 Each orthogonal treatment of [CO<sub>2</sub>] × SWC for two saplings per species was repeated twice. Each  
140 treatment lasted 7 days. One pot was exposed in each of the [CO<sub>2</sub>] × SWC treatments. Pots in the  
141 chambers were rearranged every two days to promote uniform illumination.

## 142 2.2 Foliar gas exchange measurement

143 Fully expanded primary annual leaves of the saplings were measured with a portable infrared gas  
144 photosynthesis system (LI-6400, Li-Cor, Lincoln, US) before and after the 7-day cultivation. Two  
145 saplings per species were replicated per treatment (SWC × [CO<sub>2</sub>]). For each sapling, four leaves were  
146 sampled and four measurements were conducted on each leaf. Main photosynthetic parameters, such as  
147 net photosynthetic rate (P<sub>n</sub>) and transpiration rate (T<sub>r</sub>), were measured. Based on theoretical  
148 considerations of Von Caemmerer and Farquhar (1981), stomatal conductance (g<sub>s</sub>) and intercellular  
149 [CO<sub>2</sub>] (C<sub>i</sub>) were calculated by the Li-Cor software. Instantaneous water use efficiency via gas exchange  
150 (WUE<sub>ge</sub>) was calculated as the ratio P<sub>n</sub> / T<sub>r</sub>.

## 151 2.3 Plant material collection and leaf water-soluble compounds extraction

152 Eight recently-expanded sun leaves were selected per sapling and homogenized in liquid nitrogen  
153 after gas-exchange measurements were finished. For extraction of WSCs from the leaves (Gessler et  
154 al., 2004), 50 mg of ground leaves and 100 mg of PVPP (polyvinylpolypyrrolidone) were mixed and  
155 incubated in 1 mL distilled water for 60 min at 5°C in a centrifuge tube. Each leaf sample was  
156 replicated twice. Two saplings per species were chosen for each orthogonal treatment. The tubes  
157 containing the mixture were heated in 100°C water for 3 min. After cooling to room temperature, the  
158 supernatant of the mixture was centrifuged (12000 × g for 5 min) and 10 µL of supernatant was  
159 transferred into a tin capsule and dried at 70°C. Folded capsules were used for δ<sup>13</sup>C analysis of WSCs.  
160 The samples of WSCs from leaves were combusted in an elemental analyzer (EuroEA, HEKAtech  
161 GmbH, Wegberg, Germany) and analyzed with a mass spectrometer (DELTA<sup>plus</sup>XP, ThermoFinnigan).

162 Carbon isotope signatures were expressed in δ-notation (parts per thousand), relative to the  
163 international Pee Dee Belemnite (PDB) standard:

$$164 \delta^{13}\text{C} = \left( \frac{R_{\text{sample}}}{R_{\text{standard}}} - 1 \right) \times 1000 \quad (1)$$

165 where δ<sup>13</sup>C is the heavy isotope and R<sub>sample</sub> and R<sub>standard</sub> refer to the isotope ratio between the particular

82 partly responsible for the differences in <sup>the</sup> two measurements, as it generally increases in the short term in ~~response~~ <sup>response</sup> to elevated CO<sub>2</sub> (Flexas et al., 2014), but ~~it~~ <sup>it</sup> tends to decrease under drought (Hommel et al., ~~2014~~ <sup>2014</sup>; Théroux-Rancourt et al., 2014). Therefore, it is necessary to avoid confusion between carbon ~~isotope~~ <sup>isotope</sup> discrimination derived from synthesis of soluble sugars and/or mesophyll conductance. The degree to ~~which~~ <sup>which</sup> carbon fractionation is related to environmental variation ~~has~~ <sup>has</sup> yet to be fully investigated.

88 The simultaneous isotopic analysis of leaves allows determination of temporal variation in isotopic ~~fractionation~~ <sup>fractionation</sup> (Rinne et al., 2016). This will aid ~~in~~ <sup>in</sup> the accurate recording of environmental conditions. Newly assimilated carbohydrates can be extracted, and these are termed the water-soluble compounds (WSCs) in leaves (Brandes et al., 2006; Gessler et al., 2009). WSCs can also be associated with an assimilation-weighted mean of C<sub>i</sub>/C<sub>a</sub> (and C<sub>d</sub>/C<sub>a</sub>) photosynthesized over periods ranging from a few hours to 1–2 ~~day~~ <sup>days</sup> (Pons et al., 2009). However, there is disagreement whether fractionation caused by post-carboxylation and/or mesophyll resistance can alter the stable signatures of leaf carbon and thence influence instantaneous water use efficiency (iWUE). In addition, the manner in which iWUE derived from ~~isotopic fractionation~~ <sup>isotopic fractionation</sup> responds to environmental factors, such as elevated [CO<sub>2</sub>] and/or soil water gradients, is unknown.

98 Consequently, we investigated the  $\delta^{13}\text{C}$  of fast-turnover carbohydrate pool in sapling leaves of two ~~tree~~ <sup>tree</sup> species, *Platycladus orientalis* (L.) Franco and *Quercus variabilis* Bl., native to semi-arid areas of China. We conducted gas-exchange measurements in controlled ~~environment~~ <sup>environment</sup> growth chambers ~~(FH-230, Taiwan Hipoint Corporation, Kaohsiung City, Taiwan)~~. One goal is to differentiate the <sup>13</sup>C fractionation from the site of carboxylation to cytoplasm prior to ~~sugar~~ <sup>sugar</sup> transportation in *P. orientalis* and *Q. variabilis*, that is the total <sup>13</sup>C fractionation, determined from the  $\delta^{13}\text{C}$  of WSCs and gas-exchange measurements. ~~Another~~ <sup>Another</sup> goal is to discuss the potential causes for the observed divergence, estimate contributions of post-photosynthesis and mesophyll conductance on these differences, and describe how carbon isotopic ~~fractionation~~ <sup>fractionation</sup> responds to the interactive effects of elevated [CO<sub>2</sub>] and water stress.

## 108 2 Material and Methods

### 109 2.1 Study site and design

110 *P. orientalis* and *Q. variabilis* saplings, selected as experimental material, were obtained from the Capital Circle forest ecosystem station, a part of Chinese Forest Ecosystem Research Network (CFERN), 40°03'45"N, 116°5'45"E, ~~in~~ <sup>in</sup> Beijing, China. This region is forested by *P. orientalis* and *Q. variabilis*. We chose saplings ~~of~~ <sup>of</sup> similar basal diameters, heights, and growth ~~class~~ <sup>class</sup>. Each sapling was placed into an individual pot (22 cm diam. × 22 cm high). Undisturbed soil samples were collected from the field, sieved (with particles >10 mm removed), and placed into the pots. The soil bulk density in the pots was maintained at 1.337–1.447 g·cm<sup>-3</sup>. After a ~~30-day~~ <sup>30-day</sup> transplant recovery period, the saplings were placed into growth chambers for orthogonal cultivation.

118 The controlled experiment ~~was~~ <sup>was</sup> conducted in growth chambers (FH-230, Taiwan Hipoint Corporation, Kaohsiung City, Taiwan). To reproduce the meteorological ~~conditions~~ <sup>conditions</sup> of different ~~growing~~ <sup>growing</sup> seasons in the research region, daytime and nighttime temperatures in the chambers were set to 25 ± 0.5°C from 07:00 to 17:00 and 18 ± 0.5°C from 17:00 to 07:00. Relative humidity was maintained at 60% and 80% during the daytime and nighttime, respectively. The mean daytime light intensity was 200–240 μmol·m<sup>-2</sup>·s<sup>-1</sup>. The chamber system ~~control~~ <sup>control</sup> and monitor [CO<sub>2</sub>]. Two

*is designed to both*

166 substance and the corresponding standard, respectively. The precision of repeated measurements was  
167 0.1 ‰.

## 168 2.4 Isotopic calculation

169 2.4.1 <sup>13</sup>C fractionation from the site of carboxylation to cytoplasm prior to **sugar** transportation

170 Based on the linear model of Farquhar and Sharkey (1982), the isotope discrimination,  $\Delta$ , was  
171 calculated as

$$172 \Delta = (\delta^{13}C_a - \delta^{13}C_{WSC}) / (1 + \delta^{13}C_{WSC}), \quad (2)$$

173 where  $\delta^{13}C_a$  and  $\delta^{13}C_{WSC}$  are the isotope signatures of ambient [CO<sub>2</sub>] in chambers and WSCs extracted  
174 from leaves, respectively. The  $C_i:C_a$  was determined by

$$175 C_i:C_a = (\Delta - a) / (b - a), \quad (3)$$

176 where  $C_i$  and  $C_a$  are the [CO<sub>2</sub>] within substomatal cavities and in **growth** chambers, respectively;  $a$  is  
177 the fractionation occurring CO<sub>2</sub> diffusion in still air (4‰) and  $b$  refers to the discrimination during CO<sub>2</sub>  
178 fixation by ribulose 1,5- biphosphate carboxylase/oxygenase (Rubisco) and internal diffusion (30‰).  
179 Instantaneous water use efficiency by gas-exchange **measurement** (WUE<sub>ge</sub>) was calculated as

$$180 WUE_{ge} = P_n:T_r = (C_a - C_i) / 1.6\Delta e, \quad (4)$$

181 where 1.6 is the diffusion ratio of stomatal conductance for water vapor to CO<sub>2</sub> in chambers and  $\Delta e$  is  
182 the difference between  $e_{lf}$  and  $e_{atm}$ , **representing** the extra- and intra-cellular water vapor pressure,  
183 respectively:

$$184 \Delta e = e_{lf} - e_{atm} = 0.611 \times e^{17.502T/(240.97+T)} \times (1 - RH), \quad (5)$$

185 where  $T$  and RH are the temperature and relative humidity **on leaf surface**, respectively. Combining  
186 Eqns. (2, 3 and 4), the instantaneous water use efficiency **could be determined** by the  $\delta^{13}C_{WSC}$  of leaves,  
187 defined as:

$$188 WUE_{cp} = \frac{P_n}{T_r} = (1 - \varphi) (C_a - C_i) / 1.6\Delta e = C_a(1 - \varphi) \left[ \frac{b - \delta^{13}C_a + (b+1)\delta^{13}C_{WSC}}{(b-a)(1 + \delta^{13}C_{WSC})} \right] / 1.6\Delta e, \quad (6)$$

189 where  $\varphi$  is the respiratory ratio of leaf carbohydrates to other organs at night (0.3).

190 Then the <sup>13</sup>C fractionation from the site of carboxylation to cytoplasm prior to **sugars** transportation  
191 (defined as the total <sup>13</sup>C fractionation) was estimated by the observed  $\delta^{13}C$  of WSCs from leaves  
192 ( $\delta^{13}C_{WSC}$ ) and the modeled  $\delta^{13}C$  calculated from gas-exchange measurements ( $\delta^{13}C_{model}$ ). The  $\delta^{13}C_{model}$   
193 was calculated from  $\Delta_{model}$  from Eqn. (2);  $\Delta_{model}$  was determined by **combining** Eqns. (3 and 4) as

$$194 \Delta_{model} = (b - a) \left( 1 - \frac{1.6\Delta e WUE_{ge}}{C_a} \right) + a, \quad (7)$$

$$195 \delta^{13}C_{model} = \frac{C_a - \Delta_{model}}{1 + \Delta_{model}}, \quad (8)$$

$$196 \text{Total } ^{13}\text{C fractionation} = \delta^{13}C_{WSC} - \delta^{13}C_{model}. \quad (9)$$

197 2.4.2 Method of estimations for mesophyll conductance and the contribution of post-carboxylation  
198 fractionation

199 The carbon isotope discrimination was generated from the relative contribution of diffusion and  
200 carboxylation, reflected by the ratio of [CO<sub>2</sub>] at the site of carboxylation ( $C_c$ ) to **the concentration** in the

201 outside air ( $C_a$ ). The carbon isotopic discrimination ( $\Delta$ ) can be presented as (Farquhar et al. 1982):

$$202 \quad \Delta = a_b \frac{C_a - C_s}{C_a} + a \frac{C_s - C_i}{C_a} + (e_s + a_l) \frac{C_i - C_c}{C_a} + b \frac{C_c}{C_a} - \frac{eR_D + f\Gamma^*}{C_a}, \quad (10)$$

203 where  $C_a$ ,  $C_s$ ,  $C_i$ , and  $C_c$  are the  $[\text{CO}_2]$  in the ambient air, at the boundary layer of the leaf, in the  
 204 substomatal cavities, and at the sites of carboxylation, respectively;  $a_b$  is the  $\text{CO}_2$  diffusional  
 205 fractionation at the boundary layer (2.9‰);  $e_s$  is the discrimination for  $\text{CO}_2$  diffusion when  $\text{CO}_2$  enters  
 206 in solution (1.1‰, at 25°C);  $a_l$  is the  $\text{CO}_2$  diffusional fractionation in the liquid phase (0.7‰);  $e$  and  $f$   
 207 are carbon discriminations derived in dark respiration ( $R_D$ ) and photorespiration, respectively;  $k$  is the  
 208 carboxylation efficiency, and  $\Gamma^*$  is the  $\text{CO}_2$  compensation point in the absence of dark respiration  
 209 (Brooks and Farquhar, 1985).

210 When gas in the cuvette is well stirred during gas-exchange measurements, diffusion across the  
 211 boundary layer could be neglected and Eqn. (10) can be written as

$$212 \quad \Delta = a \frac{C_a - C_i}{C_a} + (e_s + a_l) \frac{C_i - C_c}{C_a} + b \frac{C_c}{C_a} - \frac{eR_D + f\Gamma^*}{C_a}. \quad (11)$$

213 There is no consensus about the value of  $e$ , although recent measurements estimate it as ranging  
 214 from 0-4‰. The value of  $f$  has been estimated to range from 8-12‰ (Gillon and Griffiths, 1997;  
 215 Igamberdiev et al., 2004; Lanigan et al., 2008). As the most direct factor,  $b$  influences the calculation of  
 216  $g_m$ , which is thought to be approximately 30‰ in higher plants (Guy et al., 1993).

217 The difference of  $[\text{CO}_2]$  between substomatal cavities and chloroplasts is omitted, while diffusion  
 218 related to dark-respiration and photorespiration are negligible and Eqn. (11) may be simplified to

$$219 \quad \Delta_i = a + (b - a) \frac{C_i}{C_a}. \quad (12)$$

220 Eqn. (12) denotes the linear relationship between carbon discrimination and  $C_i/C_a$ . That underlines  
 221 subsequent comparison between expected  $\Delta$  (originating from gas-exchange,  $\Delta_i$ , and actually measured  
 222  $\Delta_{obs}$ ), could evaluate the differences of  $[\text{CO}_2]$  between intercellular air and sites of carboxylation that  
 223 are the  $^{13}\text{C}$  fractionation from mesophyll conductance. Consequently,  $g_m$  is calculated by subtracting the  
 224  $\Delta_{obs}$  of Eqn. (11) from  $\Delta_i$  [Eqn. (12)]:

$$225 \quad \Delta_i - \Delta_{obs} = (b - e_s - a_l) \frac{C_i - C_c}{C_a} + \frac{eR_D + f\Gamma^*}{C_a} \quad (13)$$

226 and  $P_n$  from Fick's first law is presented by

$$227 \quad P_n = g_m(C_i - C_c). \quad (14)$$

228 Substituting Eqn. (14) into Eqn. (13) we obtain

$$229 \quad \Delta_i - \Delta_{obs} = (b - e_s - a_l) \frac{P_n}{g_m C_a} + \frac{eR_D + f\Gamma^*}{C_a}, \quad \text{and} \quad (15)$$

$$230 \quad g_m = \frac{(b - e_s - a_l) \frac{P_n}{C_a}}{(\Delta_i - \Delta_{obs}) - \frac{eR_D + f\Gamma^*}{C_a}}. \quad (16)$$

231 In the calculation of  $g_m$ , terms of respiratory and photorespiratory could be ignored and  $e$  and  $f$  are  
 232 assumed to be zero or to be cancelled out in the calculation of  $g_m$ .

233 Then Eqn. (16) can be rewritten as

— these  
is no  
need for  
"S" at  
the  
end of  
[CO<sub>2</sub>]!!

234 
$$g_m = \frac{(b-e_s-a_l) \frac{P_n}{C_a}}{A_i - A_{obs}} \quad (17)$$

235 Therefore, the contribution of post- carboxylation fractionation can be estimated by

236 *Contribution of post – carboxylation fractionation =*  
 237 
$$\frac{(\text{Total }^{13}\text{C fractionation} - \text{fractionation from mesophyll conductance})}{\text{Total }^{13}\text{C fractionation}} \times 100\%. \quad (18)$$

238 **3 Results**

239 **3.1 Foliar gas exchange measurements**

240 When SWC increased between the treatments,  $P_n$ ,  $g_s$  and  $T_r$  in *P. orientalis* and *Q. variabilis* peaked  
 241 at 70%–80% of FC and/or 100% of FC (Fig. 2). The  $C_i$  in *P. orientalis* rose as SWC increased. It  
 242 peaked at 60%–70% of FC and declined thereafter with increased SWC in *Q. variabilis*. The carbon  
 243 uptake and  $C_i$  were significantly improved by elevated  $[\text{CO}_2]$  at all SWCs for the two species ( $p < 0.05$ ).  
 244 Greater increases of  $P_n$  in *P. orientalis* were found at 50%–70% of FC from  $C_{400}$  to  $C_{800}$ , which was at  
 245 35%–45% of FC in *Q. variabilis*. As water stress was reduced (at 70%–80% of FC and 100% of FC),  
 246 reduction of  $g_s$  in *P. orientalis* was more pronounced with elevated  $[\text{CO}_2]$  at a given SWC ( $p < 0.01$ ).  
 247 Nevertheless,  $g_s$  in *Q. variabilis* for  $C_{400}$ ,  $C_{500}$ , and  $C_{600}$  was significantly higher than for  $C_{800}$  at 50%–  
 248 80% of FC ( $p < 0.01$ ). Coordinated with  $g_s$ ,  $T_r$  of the two species for  $C_{400}$  and  $C_{500}$  was significantly  
 249 higher than for  $C_{600}$  and  $C_{800}$ , except at 35%–60% of FC ( $p < 0.01$ , Figs. 2g and 2h).  $P_n$ ,  $g_s$ ,  $C_i$  and  $T_r$  in  
 250 *Q. variabilis* was significantly greater than the corresponding values in *P. orientalis* ( $p < 0.01$ , Fig. 2).

251 **3.2  $\delta^{13}\text{C}$  of water-soluble compounds in leaves**

252 After observations of photosynthetic traits in leaves of the two species, the same leaves were  
 253 immediately frozen and WSCs were extracted for all orthogonal treatments. The carbon isotope  
 254 composition of WSCs ( $\delta^{13}\text{C}_{WSC}$ ) of both species increased as SWC increased (Figs. 3a and 3b,  $p < 0.01$ ).  
 255 The mean  $\delta^{13}\text{C}_{WSC}$  of *P. orientalis* and *Q. variabilis* ranged from  $-27.44 \pm 0.155\text{‰}$  to  $-26.71 \pm 0.133\text{‰}$ ,  
 256 and from  $-27.96 \pm 0.129\text{‰}$  to  $-26.49 \pm 0.236\text{‰}$ , respectively. The photosynthetic capacity varied with  
 257 increased SWC and the mean  $\delta^{13}\text{C}_{WSC}$  of the two species, reaching their respective maxima at 70%–80%  
 258 of FC. With gradual enrichment of  $[\text{CO}_2]$ , mean  $\delta^{13}\text{C}_{WSC}$  in both species declined when  $[\text{CO}_2]$  exceeded  
 259 600 ppm ( $p < 0.01$ ). Except for  $C_{400}$  at 50%–100% of FC, the  $\delta^{13}\text{C}_{WSC}$  in *P. orientalis* was significantly  
 260 larger than that in *Q. variabilis* at any  $[\text{CO}_2] \times \text{SWC}$  treatment ( $p < 0.01$ , Fig. 3).

261 **3.3 Estimations of  $\text{WUE}_{ge}$  and  $\text{WUE}_{cp}$**

262 Figure 4a shows that increments of  $\text{WUE}_{ge}$  in *P. orientalis* under severe drought (i.e., 35%–45% of  
 263 FC) were highest at any  $[\text{CO}_2]$ , ranging from 90.70% to 564.65%. The  $\text{WUE}_{ge}$  in *P. orientalis*  
 264 decreased as SWC increased, while values increased as  $[\text{CO}_2]$  increased. Differing from variation in  
 265  $\text{WUE}_{ge}$  in *P. orientalis* with moistened soil,  $\text{WUE}_{ge}$  in *Q. variabilis* increased slightly at 100% of FC  
 266 for  $C_{600}$  or  $C_{800}$  (Fig. 4b). The maximum  $\text{WUE}_{ge}$  occurred at 35%–45% of FC for  $C_{800}$  among all  
 267 orthogonal treatments associated with both species. Elevated  $[\text{CO}_2]$  enhanced the  $\text{WUE}_{ge}$  in *Q.*  
 268 *variabilis* at any SWC, except at 60%–80% of FC. Thirty-two saplings of *P. orientalis* had greater  
 269  $\text{WUE}_{ge}$  than did *Q. variabilis* for the same  $[\text{CO}_2] \times \text{SWC}$  treatments ( $p < 0.05$ ).

270 As illustrated in Fig. 5a,  $\text{WUE}_{cp}$  in *P. orientalis* for  $C_{600}$  or  $C_{800}$  increased as water stress was  
 271 alleviated beyond 50%–60% of FC, as well as that for  $C_{400}$  or  $C_{500}$ , while SWC exceeded 60%–70% of  
 272 FC. *Q. variabilis* showed variable  $\text{WUE}_{cp}$  with increasing SWC (Fig. 5b). Except for  $C_{400}$ ,  $\text{WUE}_{cp}$  in *Q.*

273 *variabilis* decreased abruptly at 50%–60% of FC, and then increased as SWC increased for  $C_{500}$ ,  $C_{600}$ ,  
274 and  $C_{800}$ . In contrast to the results for  $WUE_{ge}$ ,  $WUE_{cp}$  in *Q. variabilis* was more pronounced than in *P.*  
275 *orientalis* among all orthogonal treatments.

### 276 3.4 $^{13}C$ fractionation from the site of carboxylation to cytoplasm before sugar transportation

277 We evaluated the total  $^{13}C$  fractionation from the site of carboxylation to the cytoplasm by  
278 gas-exchange measurements and WSCs in leaves (Table 2), which can help track the path of  $^{13}C$   
279 fractionation in leaves. Comparing  $\delta^{13}C_{WSC}$  with  $\delta^{13}C_{model}$  from Eqns. (4, 7–9), the total  $^{13}C$   
280 fractionation in *P. orientalis* ranged from 0.0328‰ to 0.0472‰, which was less than that in *Q.*  
281 *variabilis* (0.0384‰ to 0.0466‰). The total fractionation in *P. orientalis* was magnified with  
282 increasing SWC especially when SWC reached 35%–80% of FC from  $C_{400}$  to  $C_{800}$  (increased by  
283 21.30%–42.04%). The total fractionation for  $C_{400}$  and  $C_{500}$  were amplified as SWC increased until  
284 50%–60% of FC in *Q. variabilis*, whereas they were increased at 50%–80% of FC and decreased at  
285 100% of FC for  $C_{600}$  and  $C_{800}$ . Elevated  $[CO_2]$  enhanced the mean total fractionation in *P. orientalis*,  
286 while fractionation in *Q. variabilis* declined sharply from  $C_{600}$  to  $C_{800}$ . Total  $^{13}C$  fractionation, with  
287 increased SWC, in *P. orientalis* increased more rapidly than it did in *Q. variabilis*.

### 288 3.5 $g_m$ imposed on the interaction of $CO_2$ concentration and water stress

289 A comparison between online leaf  $\delta^{13}C_{WSC}$  and the values of gas-exchange measurements is given to  
290 estimate the  $g_m$  over all treatments in Fig. 6 (Eqns. (10–17)). A significant increasing trend occurred in  
291  $g_m$  with decreasing water stress in *P. orientalis*, ranging from 0.0091–0.0690 mol· $CO_2$  m $^{-2}$ ·s $^{-1}$  ( $p < 0.05$ ),  
292 which reached a maximum at 100% of FC under a given  $[CO_2]$ . Increases in  $g_m$  in *Q. variabilis* with  
293 increasing SWC were not significant, except those under  $C_{400}$ . With increasing  $[CO_2]$ ,  $g_m$  in the two  
294 species increased at different rates. With *P. orientalis* under  $C_{400}$ ,  $g_m$  increased gradually and reached a  
295 maximum under  $C_{800}$  at 35%–60% of FC and 100% of FC ( $p < 0.05$ ). However, that was maximized  
296 under  $C_{600}$  ( $p < 0.05$ ) and reduced under  $C_{800}$  at 60%–80% of FC. The maximum increment in  $g_m$   
297 (8.2%–58.4%) occurred at  $C_{800}$  at all SWCs in *Q. variabilis*. The  $g_m$  in *Q. variabilis* was clearly greater  
298 than that in *P. orientalis* under the same treatments.

### 299 3.6 Contribution of post-carboxylation fractionation

300 We evaluated the difference between  $\Delta_i$  and  $\Delta_{obs}$  in  $^{13}C$  fractionation derived from mesophyll  
301 conductance. The post-photosynthetic fractionation after carboxylation can be calculated by subtracting  
302  $g_m$ -sourced fractionation from the total  $^{13}C$  fractionation (Table 2). The  $g_m$ -sourced fractionation  
303 provided a smaller contribution to the total  $^{13}C$  fractionation than did post-carboxylation fractionation  
304 irrespective of treatment (Table 2). The  $g_m$ -sourced fractionation in the two species illustrated different  
305 variations with increasing SWC, which declined at 50%–80% of FC and increased at 100% of FC in *P.*  
306 *orientalis*; yet, in *Q. variabilis*, it increased with water stress alleviation at 50%–80% of FC and then  
307 decreased at 100% of FC. Nevertheless, in the two species post-carboxylation fractionation in leaves all  
308 increased as SWC increased. The  $g_m$ -sourced fractionation in *P. orientalis* and *Q. variabilis* reached  
309 their peaks under  $C_{600}$  and  $C_{800}$ , respectively. Post-carboxylation fractionation was magnified with increases in  
310  $[CO_2]$  in *P. orientalis*, and reached a maximum under  $C_{600}$  and then declined under  $C_{800}$ .

### 311 3.7 Relationship between $g_s$ , $g_m$ and total $^{13}C$ fractionation

312 Total  $^{13}C$  fractionation may be correlated with resistances associated with stomata and mesophyll  
313 cells. We performed linear regressions between  $g_s/g_m$  and total  $^{13}C$  fractionation in *P. orientalis* and *Q.*  
314 *variabilis* (Fig. 7 and 8). The total  $^{13}C$  fractionation was correlated to  $g_s$  ( $p < 0.01$ ). The positive linear



315 relationships between  $g_m$  and total  $^{13}\text{C}$  fractionation ( $p < 0.01$ ) indicated that the variation of  $[\text{CO}_2]$   
316 through the chloroplast was correlated with carbon discrimination following leaf photosynthesis.

## 317 4 Discussion

### 318 4.1 Photosynthetic traits

319 The exchange of  $\text{CO}_2$  and water vapor via stomata can be modulated by the soil/leaf water potential  
320 (Robredo et al., 2010). Saplings of *P. orientalis* reached maximum  $P_n$  and  $g_s$  at 70%–80% of FC  
321 irrespective of  $[\text{CO}_2]$  treatments. As SWC exceeded this water threshold, elevated  $\text{CO}_2$  caused a greater  
322 reduction in  $g_s$  as <sup>was</sup> previously reported for barley and wheat (Wall et al., 2011). The decrease in  $g_s$   
323 responding to elevated  $[\text{CO}_2]$ , could be mitigated <sup>with</sup> by increased SWC. The  $C_i$  in *Q. variabilis* peaked at  
324 60%–70% of FC and then declined as soil moisture increased (Wall et al., 2006; Wall et al., 2011).  
325 This may be because stomata tend to maintain a constant  $C_i$  or  $C_i/C_a$  when ambient  $[\text{CO}_2]$  is increased,  
326 which would determine the amount of  $\text{CO}_2$  used directly in the chloroplast (Yu et al., 2010). This result  
327 could be explained as stomatal limitation (Farquhar and Sharkey, 1982; Xu, 1997). However,  $C_i$  in *P.*  
328 *orientalis* increased considerably, while SWC exceeded 70%–80% of FC, as found by Mielke et al.  
329 (2000). One possible contributing factor is plants close their stomata to reduce water loss during  
330 organic matter synthesis simultaneously decreasing the availability of  $\text{CO}_2$  and generating respiration  
331 of organic matter (Robredo et al., 2007). Another possible explanation is that the limited root volume of  
332 potted plants may be unable to absorb sufficient water to support <sup>the</sup> full growth of shoots (Leakey et al.,  
333 2009; Wall et al., 2011). In the present study, increasing  $[\text{CO}_2]$  may cause nonstomatal limitation when  
334 SWC exceeds a soil moisture threshold of 70%–80% of FC. The accumulation of nonstructural  
335 carbohydrates in leaf tissue may induce mesophyll-based and/or biochemical-based transient inhibition  
336 of photosynthetic capacity (Farquhar and Sharkey, 1982). Xu and Zhou (2011) developed a five-level  
337 SWC gradient to examine the effect of water on the physiology of perennial *Leymus chinensis*, and  
338 demonstrated that there was a clear maximum in SWC, below which the plant could adjust to changing  
339 environmental conditions. <sup>Miranda</sup> Apodaca et al. (2015) also concluded that, in suitable water <sup>seen with</sup>  
340 conditions, elevated  $\text{CO}_2$  levels augmented  $\text{CO}_2$  assimilation in herbaceous plants. <sup>ok!</sup>

341 The  $P_n$  of the two woody plant species increased with elevated  $[\text{CO}_2]$  similar to results <sup>from</sup> other  $C_3$   
342 woody plants (Kgope et al., 2010). Increasing  $[\text{CO}_2]$  alleviated severe drought and <sup>the need for</sup> heavy  
343 irrigation, suggesting that photosynthetic inhibition produced by a lack or excess of water may be  
344 mediated by increased  $[\text{CO}_2]$  (Robredo et al., 2007; Robredo et al., 2010) and ameliorate the effects of  
345 drought stress by reducing plant transpiration (Kirkham, 2016; Kadam et al., 2014; Miranda Apodaca  
346 et al., 2015; Tausz Posch et al., 2013).

### 347 4.2 Differences between $\text{WUE}_{\text{ge}}$ and $\text{WUE}_{\text{cp}}$

348 ~~The~~ increases in  $\text{WUE}_{\text{ge}}$  in *P. orientalis* and *Q. variabilis* that resulted from the combination of  $P_n$  <sup>seen with</sup>  
349 increase and  $g_s$  decrease were followed by a reduction in  $T_r$  (Figs. 2a, 2g, 2b and 2h). This result was <sup>ok!</sup>  
350 also demonstrated by Ainsworth and McGrath (2010). Comparing  $P_n$  and  $T_r$  in the two species, a lower  
351  $\text{WUE}_{\text{ge}}$  in *Q. variabilis* was obtained due to its physiological and morphological traits, such as larger  
352 leaf area, rapid growth, and higher stomatal conductance than that in *P. orientalis* (Adiredjo et al.,  
353 2014). Medlyn et al. (2001) reported that stomatal conductance of broadleaved species is more  
354 sensitive to elevated  $[\text{CO}_2]$  than conifer species. There is no agreement on the patterns of  $i\text{WUE}_l$  at the <sup>ok!</sup>  
355 leaf level, related to SWC (Yang et al., 2010). The  $\text{WUE}_{\text{ge}}$  in *P. orientalis* and *Q. variabilis* were  
356 enhanced with soil drying, as presented by Parker and Pallardy (1991), DeLucia and Heckathorn

357 (1989), Reich et al. (1989), and Leakey (2009).

358 Bögelein et al. (2012) confirmed that  $WUE_{cp}$  was more consistent with daily mean  $WUE_{ge}$  than  
359 with  $WUE_{phloem}$  (calculated <sup>with</sup> by the  $\delta^{13}C$  of phloem). The  $WUE_{cp}$  of the two species demonstrated  
360 similar variations to those in  $\delta^{13}C_{WSC}$ , which differed from those of  $WUE_{ge}$ . Pons et al. (2009) noted  
361 that  $\Delta$  of leaf soluble sugar is coupled with environmental dynamics over a period ranging from a few  
362 hours to 1–2 days. The  $WUE_{cp}$  of our materials could <sup>ed</sup> respond to  $[CO_2] \times SWC$  treatments over a  
363 number of cultivated days, whereas  $WUE_{ge}$  <sup>was</sup> is characterized as the instantaneous physiological change  
364 in plants to new conditions. Consequently,  $WUE_{cp}$  and  $WUE_{ge}$  have different degrees of variations in  
365 response to different treatments.

#### 366 4.3 Influence of mesophyll conductance on the fractionation after carboxylation

367  $CO_2$  diffusion into photosynthetic sites includes two main processes.  $CO_2$  first moves from ambient  
368 air surrounding the leaf ( $C_a$ ) through stomata to the sub-stomatic cavities ( $C_i$ ). From sub-stomatic  
369 cavities  $CO_2$  then moves to the sites of carboxylation within the chloroplast stroma ( $C_c$ ) of the leaf  
370 mesophyll. The latter procedure of diffusion is termed mesophyll conductance ( $g_m$ ; Flexas et al., 2008).  
371 Moreover,  $g_m$  has been identified to coordinate with environmental factors more rapidly than stomatal  
372 conductance (Galmés et al., 2007; Tazoe et al., 2011; Flexas et al., 2007). During our 7-day cultivations  
373 of  $SWC \times [CO_2]$ ,  $g_m$  increased and  $WUE_{ge}$  decreased with increasing SWC. It has been documented  
374 that  $g_m$  can improve WUE under drought pretreatment (Han et al., 2016). However, the mechanism <sup>by</sup>  
375 which  $g_m$  responds to the fluctuation of  $[CO_2]$  is unclear. Terashima et al. (2006) demonstrated that  
376  $CO_2$  permeable aquaporin, located in the plasma membrane and inner envelope of chloroplasts, could  
377 regulate the change in  $g_m$ . In our study,  $g_m$  is species-specific to the  $[CO_2]$  gradient. The  $g_m$  in *P.*  
378 *orientalis* significantly decreased by 9.08%–44.42% from  $C_{600}$  to  $C_{800}$  at 60%–80% of FC; these are  
379 similar to the results of Flexas et al. (2007). A larger  $g_m$  in *Q. variabilis* under  $C_{800}$  was observed  
380 compared <sup>to</sup> with *P. orientalis*.

381 Furthermore,  $g_m$  contributed to the total  $^{13}C$  fractionation that followed carboxylation, while  
382 photosynthate had not been transported to the sapling twigs. The  $^{13}C$  fractionation of  $CO_2$  from the air  
383 surrounding the leaf to sub-stomatic cavities may be simply explained by stomatal resistance, which  
384 also contains the fractionation derived from mesophyll conductance between sub-stomatic cavities and  
385 the site of carboxylation in the chloroplast that cannot be neglected and should be <sup>??</sup> included (Pons et  
386 al., 2009; Cano et al., 2014). In estimating the post-carboxylation fractionation,  $g_m$ -sourced  
387 fractionation must be subtracted from the total  $^{13}C$  fractionation (the difference between  $\delta^{13}C_{WSC}$  and  
388  $\delta^{13}C_{model}$ ), which is closely associated with  $g_m$  (Fig. 8,  $p = 0.01$ ). Variations in  $g_m$ -sourced fractionation  
389 are coordinated with those in  $g_m$  with changing environmental conditions (Table 2).

#### 390 4.4 Post-carboxylation fractionation generated before photosynthate moves out of leaves

391 Photosynthesis, a biochemical and physiological process (Badeck et al., 2005), is characterized by  
392 discrimination in  $^{13}C$ , which leaves an isotopic signature in the photosynthetic apparatus. Farquhar et al.  
393 (1989) reviewed the carbon-fractionation in leaves and covered the significant aspects of  
394 photosynthetic carbon isotope discrimination. The post-carboxylation/photosynthetic fractionation  
395 associated with the metabolic pathways of non-structural carbohydrates (NSC; defined here as soluble  
396 sugars + starch) within leaves, and fractionation during translocation, storage, and remobilization prior  
397 to tree ring formation is unclear (Epron et al., 2012; Gessler et al., 2014; Rinne et al., 2016). The  
398 synthesis of sucrose and starch before transportation to twigs falls within the domain of  
399 post-carboxylation fractionation generated in leaves. Hence, we hypothesized that  $^{13}C$  fractionation

comes  
~~stays~~  
late to  
in the  
text; should  
have been  
referred  
to earlier

— X  
wrong  
word —  
"elucidated"  
maybe?

400 might exist. When we completed the leaf gas-exchange measurements, leaf samples were collected  
401 immediately to determine the  $\delta^{13}\text{C}_{WSC}$ . Presumably,  $^{13}\text{C}$  fractionation generated in the synthetic  
402 processes of sucrose and starch was contained within the  $^{13}\text{C}$  fractionation from the site of  
403 carboxylation to cytoplasm before **sugar** transportation. Comparing  $\delta^{13}\text{C}_{WSC}$  with  $\delta^{13}\text{C}_{obs}$ , the total  $^{13}\text{C}$   
404 fractionation in *P. orientalis* ranged from 0.0328‰ to 0.0472‰, which was somewhat less than that in  
405 *Q. variabilis* (from 0.0384‰ to 0.0466‰). Post-carboxylation fractionation contributed 75.30%–98.9%  
406 to total  $^{13}\text{C}$  fractionation, determined by subtracting the fractionation in  $g_m$  from total  $^{13}\text{C}$  fractionation.  
407 Gessler et al. (2004) reviewed the environmental components of variation in photosynthetic carbon  
408 isotope discrimination in terrestrial plants. Total  $^{13}\text{C}$  fractionation in *P. orientalis* was enhanced by the  
409 increase in SWC, consistent with that in *Q. variabilis*, except at 100% of FC. The  $^{13}\text{C}$  isotope signature  
410 in *P. orientalis* was depleted with elevated  $[\text{CO}_2]$ . Yet,  $^{13}\text{C}$ -depletion was weakened in *Q. variabilis* for  
411  $C_{600}$  and  $C_{800}$ . Linear regressions between  $g_s$  and total  $^{13}\text{C}$  fractionation indicated that the  
412 post-carboxylation fractionation in leaves depends on the variation of  $g_s$  and **that stomata** aperture was  
413 correlated with environmental change.

## 414 5 Conclusions

415 Through orthogonal treatments of four  $[\text{CO}_2]$   $\times$  five SWCs,  $\text{WUE}_{cp}$  calculated by  $\delta^{13}\text{C}_{WSC}$  and  
416  $\text{WUE}_{ge}$  derived from simultaneous leaf gas-exchange, were estimated to differentiate the  $\delta^{13}\text{C}$  signal  
417 variation before leaf-level translocation of primary assimilates. The influence of  $g_m$  on  $^{13}\text{C}$  fractionation  
418 between the sites of carboxylation and **ambient air** is important. It requires consideration when testing  
419 the hypothesis that the post-carboxylation contributes to the  $^{13}\text{C}$  fractionation from the site of  
420 carboxylation to cytoplasm before **sugar** transport. In response to the interactive effects of  $[\text{CO}_2]$  and  
421 SWC,  $\text{WUE}_{ge}$  in the two tree species both decreased with increasing SWC, and increased with elevated  
422  $[\text{CO}_2]$  at 35%–80% of FC. We concluded that relative soil drying, coupled with elevated  $[\text{CO}_2]$ , can  
423 improve  $\text{WUE}_{ge}$  by strengthening photosynthetic capacity and reducing transpiration.  $\text{WUE}_{ge}$  in *P.*  
424 *orientalis* was significantly greater than that in *Q. variabilis*, while the opposite was the case for  
425  $\text{WUE}_{cp}$ . The  $g_m$  and post-carboxylation both contributed to the total  $^{13}\text{C}$  fractionation. **Rising**  $[\text{CO}_2]$   
426 and/or moistening soil generated increasing disparities between  $\delta^{13}\text{C}_{WSC}$  and  $\delta^{13}\text{C}_{model}$  in *P. orientalis*;  
427 nevertheless, the differences between  $\delta^{13}\text{C}_{WSC}$  and  $\delta^{13}\text{C}_{model}$  in *Q. variabilis* increased when  $[\text{CO}_2]$  was  
428 less than 600 ppm and/or water stress was alleviated. Total  $^{13}\text{C}$  fractionation in **the** leaf was linearly  
429 dependent on  $g_s$ . With respect to carbon isotope fractionation in post-carboxylation and transportation  
430 processes, we note that  $^{13}\text{C}$  fractionation derived from the synthesis of sucrose and starch is likely  
431 influenced by environmental changes. A clear description of the magnitude and environmental  
432 dependence of post-carboxylation fractionation is worth **considering**.

## 433 References

- 434 Adiredjo, A. L., Navaud, O., Lamaze, T., and Grieu, P.: Leaf carbon isotope discrimination as an  
435 accurate indicator of water use efficiency in sunflower genotypes subjected to five stable soil  
436 water contents, *J Agron. Crop Sci.*, 200, 416–424, 2014.
- 437 Ainsworth, E. A. and McGrath, J. M.: Direct effects of rising atmospheric carbon dioxide and ozone on  
438 crop yields, *Climate Change and Food Security*, Springer, 109–130, 2010.
- 439 Badeck, F. W., Tcherkez, G., Eacute, N. S. S., Piel, C. E. M., and Ghashghaie, J.: Post-photosynthetic  
440 fractionation of stable carbon isotopes between plant organ – a widespread phenomenon, *Rapid*

441 Commun. Mass S., 19, 1381–1391, 2005.

442 Bögelein, R., Hassdenteufel, M., Thomas, F. M., and Werner, W.: Comparison of leaf gas exchange  
443 and stable isotope signature of water-soluble compounds along canopy gradients of co-occurring  
444 Douglas-fir and European beech, *Plant Cell Environ.*, 35, 1245–1257, 2012.

445 Brandes, E., Kodama, N., Whittaker, K., Weston, C., Rennenberg, H., Keitel, C., Adams, M. A., and  
446 Gessler, A.: Short-term variation in the isotopic composition of organic matter allocated from the  
447 leaves to the stem of *Pinus sylvestris*: effects of photosynthetic and postphotosynthetic carbon  
448 isotope fractionation, *Global Change Biol.*, 12, 1922–1939, 2006.

449 Brooks, A. and Farquhar, G. D.: Effect of temperature on the CO<sub>2</sub>/O<sub>2</sub> specificity of  
450 ribulose-1,5-bisphosphate carboxylase/oxygenase and the rate of respiration in the light, *Planta*,  
451 165, 397–406, 1985.

452 Brugnoli E, Farquhar GD. 2000. Photosynthetic fractionation of carbon isotopes. In: Leegood RC,  
453 Sharkey TD, von Caemmerer S. eds. Photosynthesis: physiology and metabolism. Advances in  
454 photosynthesis. Dordrecht, The Netherlands: Kluwer Academic Publishers, 399–434.

455 Cano, F. J., López, R., and Warren, C. R.: Implications of the mesophyll conductance to CO<sub>2</sub> for  
456 photosynthesis and water-use efficiency during long-term water stress and recovery in two  
457 contrasting Eucalyptus species, *Plant Cell Environ.*, 37, 2470–2490, 2014.

458 Cernusak, L. A., Ubierna, N., Winter, K., Holtum, J. A. M., Marshall, J. D., and Farquhar, G. D.:  
459 Environmental and physiological determinants of carbon isotope discrimination in terrestrial  
460 plants, *New Phytologist*, 200, 950–965, 2013.

461 DeLucia, E. H. and Heckathorn, S. A.: The effect of soil drought on water-use efficiency in a  
462 contrasting Great Basin desert and Sierran montane species, *Plant Cell Environ.*, 12, 935–940,  
463 1989.

464 Epron, D., Nouvellon, Y., and Ryan, M. G.: Introduction to the invited issue on carbon allocation of  
465 trees and forests, *Tree physiol.*, 32, 639–643, 2012.

466 Evans, J. R., Kaldenhoff, R., Genty, B., and Terashima, I.: Resistances along the CO<sub>2</sub> diffusion  
467 pathway inside leaves, *J. Exp. Bot.*, 60, 2235–2248, 2009.

468 Evans, J. R., Sharkey, T. D., Berry, J. A., and Farquhar, G. D.: Carbon isotope discrimination measured  
469 concurrently with gas-exchange to investigate CO<sub>2</sub> diffusion in leaves of higher-plants, *Funct.*  
470 *Plant Biol.*, 13, 281–292, 1986.

471 Evans, J. R. and von Caemmerer, S.: Temperature response of carbon isotope discrimination and  
472 mesophyll conductance in tobacco, *Plant Cell Environ.*, 36, 745–756, 2013.

473 Farquhar, G. D., Ehleringer, J. R., and Hubick, K. T.: Carbon isotope discrimination and  
474 photosynthesis, *Ann. Rev. Plant Physiol.*, 40, 503–537, 1989.

475 Farquhar, G. D., O'Leary, M. H., and Berry, J. A.: On the relationship between carbon isotope  
476 discrimination and the intercellular carbon dioxide concentration in leaves, *Funct. Plant Biol.*, 9,  
477 121–137, 1982.

478 Farquhar, G. D. and Sharkey, T. D.: Stomatal conductance and photosynthesis, *Ann. Rev. Plant*  
479 *Physiol.*, 33, 317–345, 1982.

480 Flexas, J., Barbour, M. M., Brendel, O., Cabrera, H. M., Carriquí, M., Díaz-Espejo, A., Douthe, C.,  
481 Dreyer, E., Ferrio, J. P., Gago, J., Gallé, A., Galmés, J., Kodama, N., Medrano, H., Niinemets, Ü.,  
482 Peguero-Pina, J. J., Pou, A., Ribas-Carbó, M., Tomás, M., Tosens, T., and Warren, C. R.:  
483 Mesophyll diffusion conductance to CO<sub>2</sub>: An unappreciated central player in photosynthesis, *Plant*  
484 *Science*, 193–194, 70–84, 2012.

485 Flexas, J., Carriquí, M., Coopman, R. E., Gago, J., Galmés, J., Martorell, S., Morales, F., and  
486 Diaz-Espejo, A.: Stomatal and mesophyll conductances to CO<sub>2</sub> in different plant groups:  
487 Underrated factors for predicting leaf photosynthesis responses to climate change? *Plant Science*,  
488 226, 41–48, 2014.

489 Flexas, J., Diaz-Espejo, A., Galmés, J., Kaldenhoff, R., Medano, H., and Ribas-Carbo, M.: Rapid  
490 variations of mesophyll conductance in response to changes in CO<sub>2</sub> concentration around leaves,  
491 *Plant Cell Environ.*, 30, 1284–1298, 2007.

492 Flexas, J., Ribas-Carbó, M., Diaz-Espejo, A., Galmés, J., and Medrano, H.: Mesophyll conductance to  
493 CO<sub>2</sub>: current knowledge and future prospects, *Plant Cell Environ.*, 31, 602–621, 2008.

494 Flexas, J., Ribas-Carbó, M., Hanson, D.T., Bota, J., Otto, B., Cifre, J., McDowell, N., Medrano, H., and  
495 Kaldenhoff, R.: Tobacco aquaporin NtAQP1 is involved in mesophyll conductance to CO<sub>2</sub> *in vivo*,  
496 *Plant J.*, 48, 427–439, 2006.

497 Galmés, J., Medrano, H., and Flexas, J.: Photosynthetic limitations in response to water stress and  
498 recovery in Mediterranean plants with different growth forms, *New Phytol.*, 175, 81–93, 2007.

499 Gessler, A., Brandes, E., Buchmann, N., Helle, G., Rennenberg, H., and Barnard, R. L.: Tracing carbon  
500 and oxygen isotope signals from newly assimilated sugars in the leaves to the tree-ring archive,  
501 *Plant Cell Environ.*, 32, 780–795, 2009.

502 Gessler, A., Ferrio, J. P., Hommel, R., Treydte, K., Werner, R. A., and Monson, R. K.: Stable isotopes  
503 in tree rings: towards a mechanistic understanding of isotope fractionation and mixing processes  
504 from the leaves to the wood, *Tree Physiol.*, 34, 796–818, 2014.

505 Gessler, A., Rennenberg, H., and Keitel, C.: Stable isotope composition of organic compounds  
506 transported in the phloem of European beech-evaluation of different methods of phloem sap  
507 collection and assessment of gradients in carbon isotope composition during leaf-to-stem transport,  
508 *Plant Biology*, 6, 721–729, 2004.

509 Gessler, A., Tcherkez, G., Peuke, A. D., Ghashghaie, J., and Farquhar, G. D.: Experimental evidence  
510 for diel variations of the carbon isotope composition in leaf, stem and phloem sap organic matter  
511 in *Ricinus communis*, *Plant Cell Environ.*, 31, 941–953, 2008.

512 Gillon, J. S., Griffiths, H.: The influence of (photo)respiration on carbon isotope discrimination in  
513 plants. *Plant Cell Environ.*, 20, 1217–1230, 1997.

514 Gleixner, G. and Schmidt, H.: Carbon isotope effects on the fructose-1, 6-bisphosphate aldolase  
515 reaction, origin for non-statistical <sup>13</sup>C distributions in carbohydrates, *J. Biol. Chem.*, 272, 5382–  
516 5387, 1997.

517 Guy, R. D., Fogel, M. L., and Berry, J. A.: Photosynthetic fractionation of the stable isotopes of oxygen  
518 and carbon, *Plant Physiol.*, 101, 37–47, 1993.

519 Han, J. M., Meng, H. F., Wang, S. Y., Jiang, C. D., Liu, F., Zhang, W. F., and Zhang, Y. L.: Variability  
520 of mesophyll conductance and its relationship with water use efficiency in cotton leaves under  
521 drought pretreatment, *J. Plant Physiol.*, 194, 61–71, 2016.

522 Hommel, R., Siegwolf, R., Saurer, M., Farquhar, G. D., Kayler, Z., Ferrio, J. P., and Gessler, A.:  
523 Drought response of mesophyll conductance in forest understory species-impacts on water-use  
524 efficiency and interactions with leaf water movement, *Physiol. Plantarum*, 152, 98–114, 2014.

525 Igamberdiev, A. U., Mikkelsen, T. N., Ambus, P., Bauwe, H., and Lea, P. J.: Photorespiration  
526 contributes to stomatal regulation and carbon isotope fractionation: a study with barley, potato and  
527 Arabidopsis plants deficient in glycine decarboxylase, *Photosynth. Res.*, 81, 139–152, 2004.

528 IPCC: Summary for policymakers, in: *Climate Change 2014, Mitigation of Climate Change*,

529 contribution of Working Group III to the Fifth Assessment Report of the Intergovernmental Panel  
530 on Climate Change, edited by: Edenhofer, O., Pichs-Madruga, R., Sokona, Y., Farahani, E.,  
531 Kadner, S., Seyboth, K., Adler, A., Baum, I., Brunner, S., Eickemeier, P., Kriemann, B.,  
532 Savolainen, J., Schlomer, S., von Stechow, C., Zwickel, T., and Minx, J. C., Cambridge  
533 University Press, Cambridge, UK and New York, NY, USA, 1–30, 2014.

534 Jäggi, M., Saurer, M., Fuhrer, J., and Siegwolf, R.: The relationship between the stable carbon isotope  
535 composition of needle bulk material, starch, and tree rings in *Picea abies*, *Oecologia*, 131, 325–  
536 332, 2002.

537 Kadam, N. N., Xiao, G., Melgar, R. J., Bahuguna, R. N., Quinones, C., Tamilselvan, A., Prasad, P. V.  
538 V., and Jagadish, K. S. V.: Chapter three-agronomic and physiological responses to high  
539 temperature, drought, and elevated CO<sub>2</sub> interactions in cereals, *Adv. Agron.*, 127, 111–156, 2014.

540 Kgope, B. S., Bond, W. J., and Midgley, G. F.: Growth responses of African savanna trees implicate  
541 atmospheric [CO<sub>2</sub>] as a driver of past and current changes in savanna tree cover, *Austral Ecol.*, 35,  
542 451–463, 2010.

543 Kirkham, M. B.: Elevated carbon dioxide: impacts on soil and plant water relations, CRC Press,  
544 London, New York, 2016.

545 Kodama, N., Barnard, R. L., Salmon, Y., Weston, C., Ferrio, J. P., Holst, J., Werner, R. A., Saurer, M.,  
546 Rennenberg, H., and Buchmann, N.: Temporal dynamics of the carbon isotope composition in a  
547 *Pinus sylvestris* stand: from newly assimilated organic carbon to respired carbon dioxide,  
548 *Oecologia*, 156, 737–750, 2008.

549 Lanigan, G. J., Betson, N., Griffiths, H., and Seibt, U.: Carbon isotope fractionation during  
550 photorespiration and carboxylation in *Senecio*, *Plant Physiol.*, 148, 2013–2020, 2008.

551 Le Roux, X., Bariac, T., Sinoquet H., Genty, B., Piel, C., Mariotti, A., Girardin, C., and Richard, P.:  
552 Spatial distribution of leaf water-use efficiency and carbon isotope discrimination within an  
553 isolated tree crown, *Plant Cell Environ.*, 24, 1021–1032, 2001.

554 Leakey, A. D.: Rising atmospheric carbon dioxide concentration and the future of C4 crops for food  
555 and fuel, *Proceedings of the Royal Society of London B: Biological Sciences*, 276, 1517–2008,  
556 2009.

557 Leakey, A. D., Ainsworth, E. A., Bernacchi, C. J., Rogers, A., Long, S. P., and Ort, D. R.: Elevated  
558 CO<sub>2</sub> effects on plant carbon, nitrogen, and water relations: six important lessons from FACE, *J.*  
559 *Exp. Bot.*, 60, 2859–2876, 2009.

560 Lobell, D. B., Roberts, M. J., Schlenker, W., Braun, N., Little, B. B., Rejesus, R. M., and Hammer, G.  
561 L.: Greater sensitivity to drought accompanies maize yield increase in the US Midwest, *Science*,  
562 344, 516–519, 2014.

563 Medlyn, B. E., Barton, C. V. M., Broadmeadow, M. S. J., Ceulemans, R., Angelis, P. D., Forstreuter,  
564 M., Freeman, M., Jackson, S. B., Kellomäki, S., and Laitat, E.: Stomatal conductance of forest  
565 species after long-term exposure to elevated CO<sub>2</sub> concentration: a synthesis, *New Phytol.*, 149,  
566 247–264, 2001.

567 Mielke, M. S., Oliva, M. A., de Barros, N. F., Penchel, R. M., Martinez, C. A., Da Fonseca, S., and de  
568 Almeida, A. C.: Leaf gas exchange in a clonal eucalypt plantation as related to soil moisture, leaf  
569 water potential and microclimate variables, *Trees*, 14, 263–270, 2000.

570 Miranda Apodaca, J., Pérez López, U., Lacuesta, M., Mena Petite, A., and Muñoz Rueda, A.: The type  
571 of competition modulates the ecophysiological response of grassland species to elevated CO<sub>2</sub> and  
572 drought, *Plant Biolog.*, 17, 298–310, 2015.

573 Parker, W. C. and Pallardy, S. G.: Gas exchange during a soil drying cycle in seedlings of four black  
574 walnut (*Juglans nigra* L.) Families, *Tree physiol.*, 9, 339–348, 1991.

575 Pons, T. L., Flexas, J., von Caemmerer, S., Evans, J. R., Genty, B., Ribas-Carbo, M., and Brugnoli, E.:  
576 Estimating mesophyll conductance to CO<sub>2</sub>: methodology, potential errors, and recommendations,  
577 *J. Exp. Bot.*, 8, 1–18, 2009.

578 Reich, P. B., Walters, M. B., and Tabone, T. J.: Response of *Ulmus americana* seedlings to varying  
579 nitrogen and water status. 2 Water and nitrogen use efficiency in photosynthesis, *Tree Physiol.*, 5,  
580 173–184, 1989.

581 Rinne, K. T., Saurer, M., Kirilyanov, A. V., Bryukhanova, M. V., Prokushkin, A. S., Churakova  
582 Sidorova, O. V., and Siegwolf, R. T.: Examining the response of larch needle carbohydrates to  
583 climate using compound-specific δ<sup>13</sup>C and concentration analyses, EGU General Assembly  
584 Conference, 1814949R, 2016.

585 Robredo, A., Pérez-López, U., de la Maza, H. S., González-Moro, B., Lacuesta, M., Mena-Petite, A.,  
586 and Muñoz-Rueda, A.: Elevated CO<sub>2</sub> alleviates the impact of drought on barley improving water  
587 status by lowering stomatal conductance and delaying its effects on photosynthesis, *Environ. Exp.*  
588 *Bot.*, 59, 252–263, 2007.

589 Robredo, A., Pérez-López, U., Lacuesta, M., Mena-Petite, A., and Muñoz-Rueda, A.: Influence of  
590 water stress on photosynthetic characteristics in barley plants under ambient and elevated CO<sub>2</sub>  
591 concentrations, *Biologia. Plantarum*, 54, 285–292, 2010.

592 Rossmann, A., Butzenlechner, M., and Schmidt, H.: Evidence for a nonstatistical carbon isotope  
593 distribution in natural glucose, *Plant Physiol.*, 96, 609–614, 1991.

594 Streit, K., Rinne, K. T., Hagedorn, F., Dawes, M. A., Saurer, M., Hoch, G., Werner, R. A., Buchmann,  
595 N., and Siegwolf, R. T. W.: Tracing fresh assimilates through *Larix decidua* exposed to elevated  
596 CO<sub>2</sub> and soil warming at the alpine treeline using compound-specific stable isotope analysis, *New*  
597 *Phytol.*, 197, 838–849, 2013.

598 Tausz Posch, S., Norton, R. M., Seneweera, S., Fitzgerald, G. J., and Tausz, M.: Will intra-specific  
599 differences in transpiration efficiency in wheat be maintained in a high CO<sub>2</sub> world? A FACE study,  
600 *Physiol. Plantarum*, 148, 232–245, 2013.

601 Tazoe, Y., von Caemmerer, S., Estavillo, G. M., and Evans, J. R.: Using tunable diode laser  
602 spectroscopy to measure carbon isotope discrimination and mesophyll conductance to CO<sub>2</sub>  
603 diffusion dynamically at different CO<sub>2</sub> concentrations, *Plant Cell Environ.*, 34, 580–591, 2011.

604 Terashima, I., Hanba, Y.T., Tazoe, Y., Vyas, P., and Yano, S.: Irradiance and phenotype: comparative  
605 eco-development of sun and shade leaves in relation to photosynthetic CO<sub>2</sub> diffusion, *J. Exp. Bot.*,  
606 57, 343–354, 2006.

607 Thérroux-Rancourt, G., Éthier, G., and Pepin, S.: Threshold response of mesophyll CO<sub>2</sub> conductance to  
608 leaf hydraulics in highly transpiring hybrid poplar clones exposed to soil drying, *J. Exp. Bot.*, 65,  
609 741–753, 2014.

610 Von Caemmerer, S. V. and Farquhar, G. D.: Some relationships between the biochemistry of  
611 photosynthesis and the gas exchange of leaves, *Planta*, 153, 376–387, 1981.

612 Wall, G. W., Garcia, R. L., Kimball, B. A., Hunsaker, D. J., Pinter, P. J., Long, S. P., Osborne, C. P.,  
613 Hendrix, D. L., Wechsung, F., and Wechsung, G.: Interactive effects of elevated carbon dioxide  
614 and drought on wheat, *Agron. J.*, 98, 354–381, 2006.

615 Wall, G. W., Garcia, R. L., Wechsung, F., and Kimball, B. A.: Elevated atmospheric CO<sub>2</sub> and drought  
616 effects on leaf gas exchange properties of barley, *Agr. Ecosyst. Environ.*, 144, 390–404, 2011.

617 Warren, C. R. and Adams, M. A.: Internal conductance does not scale with photosynthetic capacity:  
618 implications for carbon isotope discrimination and the economics of water and nitrogen use in  
619 photosynthesis, *Plant Cell Environ.*, 29, 192–201, 2006.  
620 Xu, D. Q.: Some problems in stomatal limitation analysis of photosynthesis, *Plant Physiol. J.*, 33, 241–  
621 244, 1997.  
622 Xu, Z. and Zhou, G.: Responses of photosynthetic capacity to soil moisture gradient in perennial  
623 rhizome grass and perennial bunchgrass, *BMC Plant Boil.*, 11, 21, 2011.  
624 Yang, B., Pallardy, S. G., Meyers, T. P., GU, L. H., Hanson, P. J., Wullschleger, S. D., Heuer, M.,  
625 Hosman, K. P., Riggs, J. S., and Sluss D. W.: Environmental controls on water use efficiency  
626 during severe drought in an Ozark Forest in Missouri, USA, *Global Change Biol.*, 16, 2252–2271,  
627 2010.  
628 Yu, G., Wang, Q., and Mi, N.: *Ecophysiology of plant photosynthesis, transpiration, and water use*,  
629 Science Press, Beijing, China, 2010.

630

631 **Author contributions**

632 N. Zhao and Y. He collected field samples, and performed experiments. N. Zhao ~~performed data~~  
633 ~~analysis~~ and wrote the paper. P. Meng commented on the theory and study design. X. Yu revised and  
634 edited the manuscript.

*the*  
*analysed the data*

635

636 *Acknowledgements.* Financial support for this project was provided by the National Natural Science  
637 Foundation of China (grant No. 41430747) and the Beijing Municipal Education Commission  
638 (CEFF-PXM2017\_014207\_000043). We thank Beibei Zhou and Yuanhai Lou for collection of  
639 materials and management of saplings. We are grateful to anonymous reviewers for constructive  
640 suggestions regarding this manuscript. Due to space limitations we cited selected references involving  
641 this study topic and apologize for authors whose work was not cited.

642

643

644

645

646

647

648

649

650

651

652

653

654

655

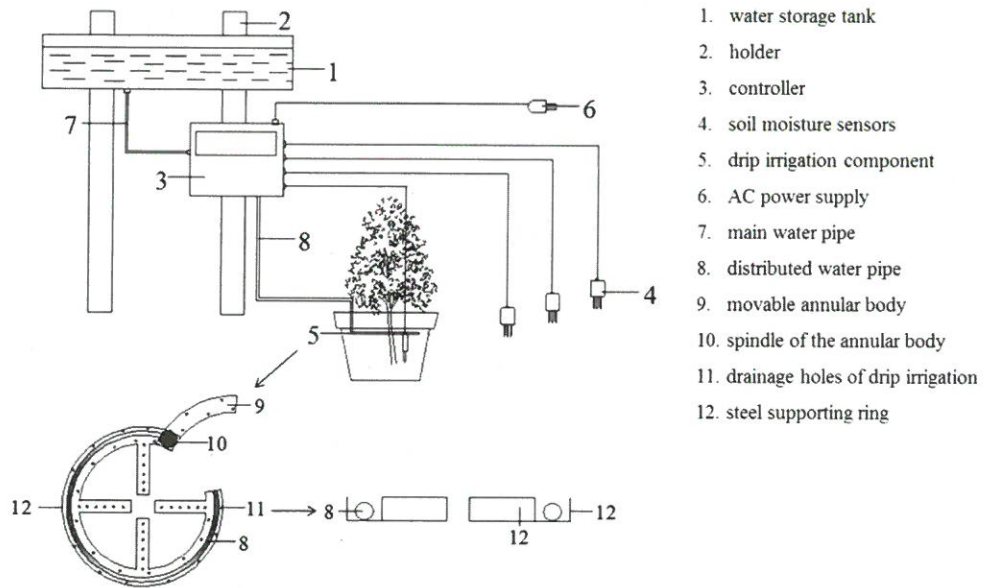
656

657

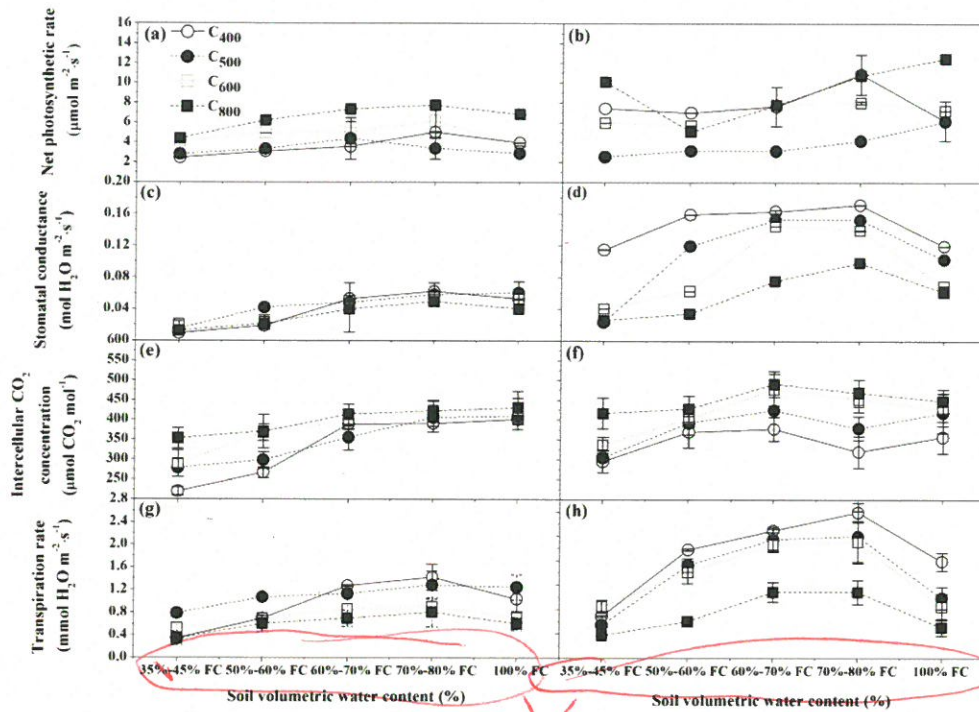
658

659



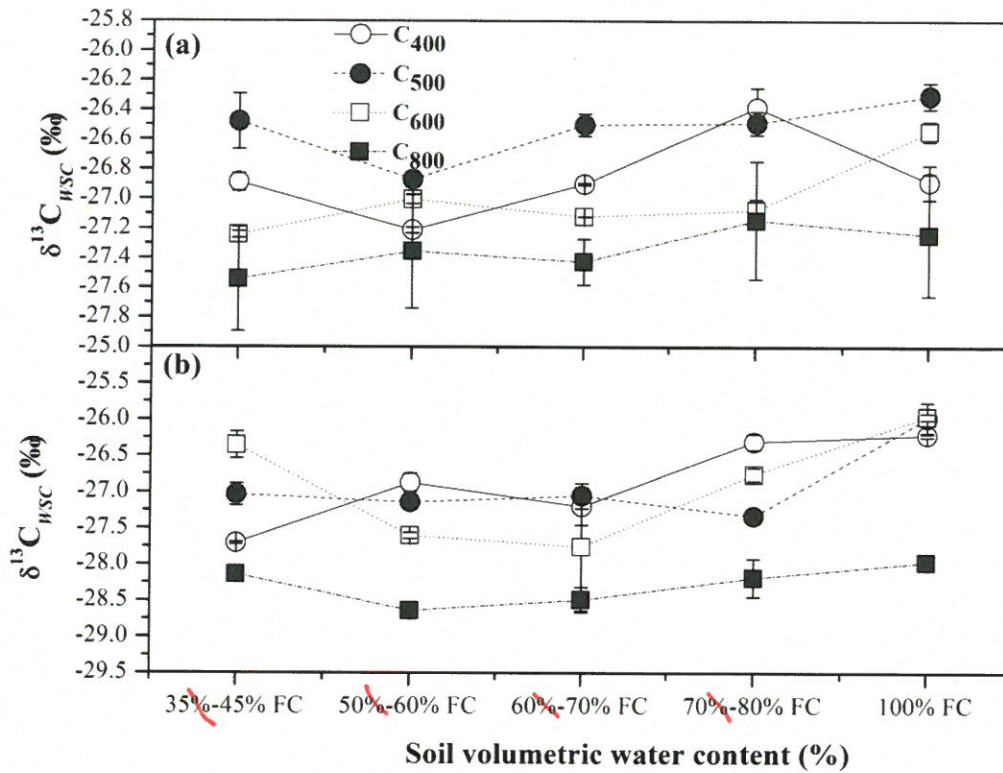


661 **Figure 1.** Diagram of the automatic drip irrigation device used in this study; numbers indicate the  
 662 individual parts of the irrigation device (No. 1–12). The lower-left corner of this figure presents the  
 663 detailed schematic for the drip irrigation component (No. 8–12).

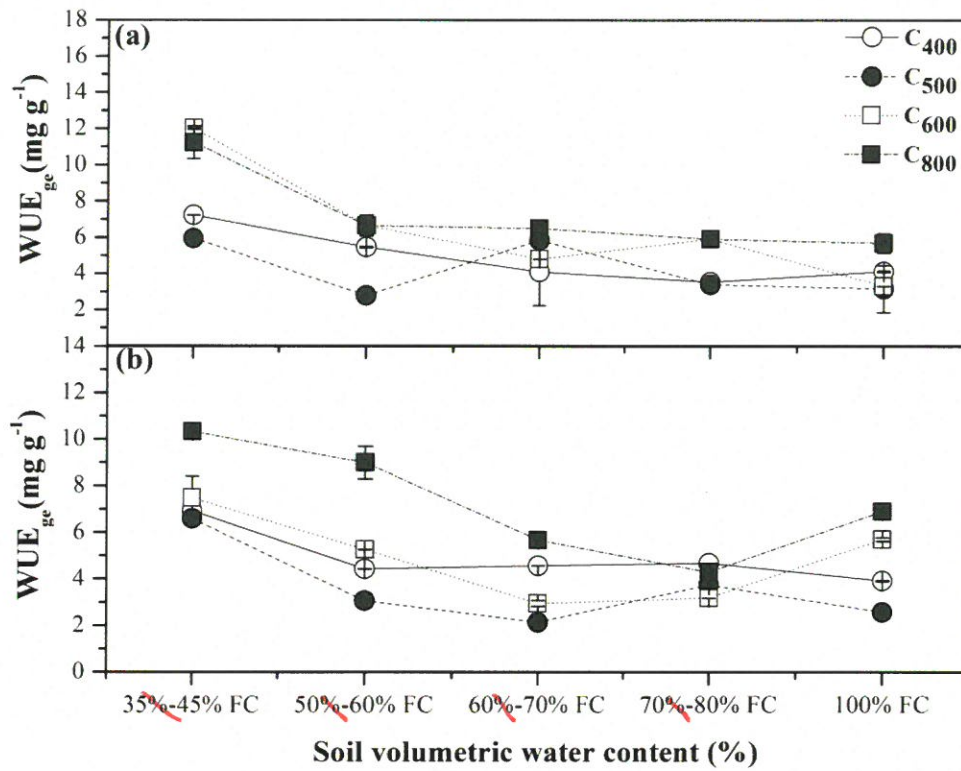


Simplify the labels; Also too small.

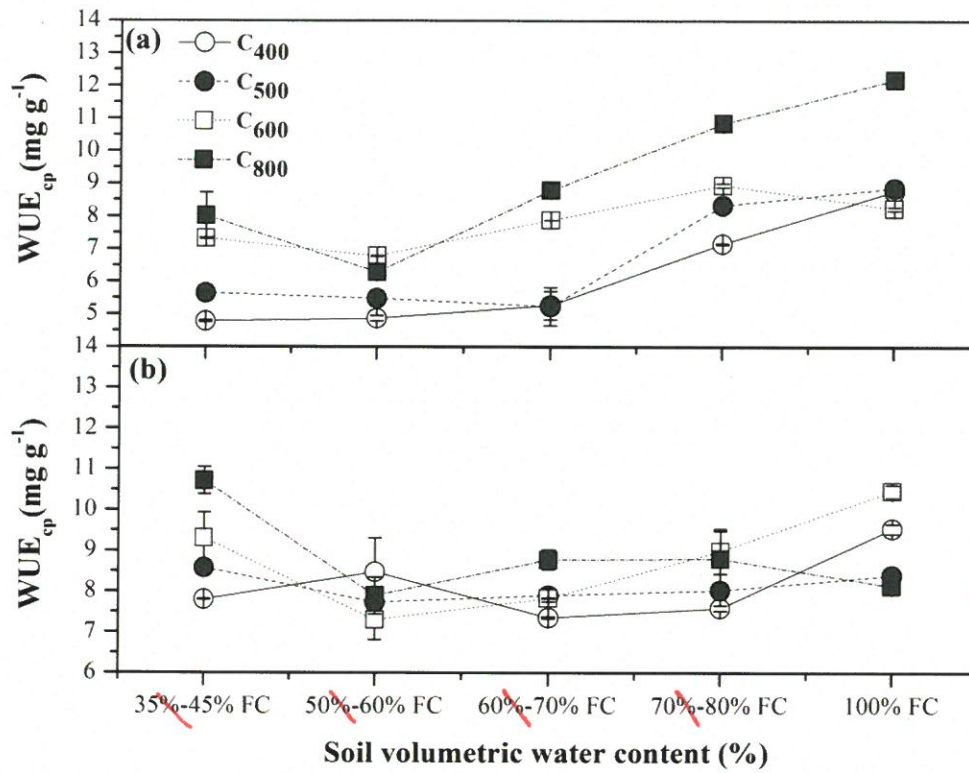
664 **Figure 2.** Net photosynthetic rates ( $P_n$ ,  $\mu\text{mol m}^{-2} \text{s}^{-1}$ , a and b), stomatal conductance ( $g_s$ ,  $\text{mol H}_2\text{O m}^{-2}$   
 665  $\text{s}^{-1}$ , c and d), intercellular  $\text{CO}_2$  concentration ( $C_i$ ,  $\mu\text{mol CO}_2 \text{mol}^{-1}$ , e and f), and transpiration rates ( $T_r$ ,  
 666  $\text{mmol H}_2\text{O m}^{-2} \text{s}^{-1}$ , g and h) in *P. orientalis* and *Q. variabilis* for four  $\text{CO}_2$  concentrations  $\times$  five soil  
 667 volumetric water content treatments. Means  $\pm$  SDs,  $n=32$ .



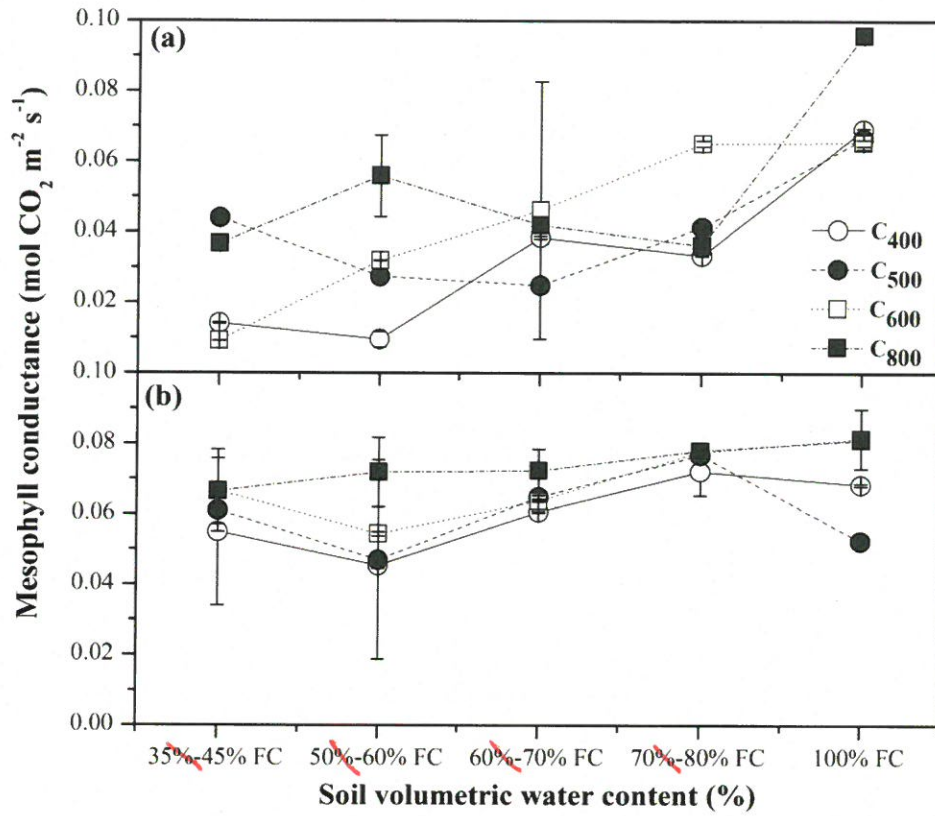
668 **Figure 3.** Carbon isotope composition of water-soluble compounds ( $\delta^{13}C_{WSC}$ ) extracted from leaves of  
 669 *P. orientalis* (a) and *Q. variabilis* (b) for four CO<sub>2</sub> concentrations  $\times$  five soil volumetric water content  
 670 treatments. Means  $\pm$  SDs, n= 32.



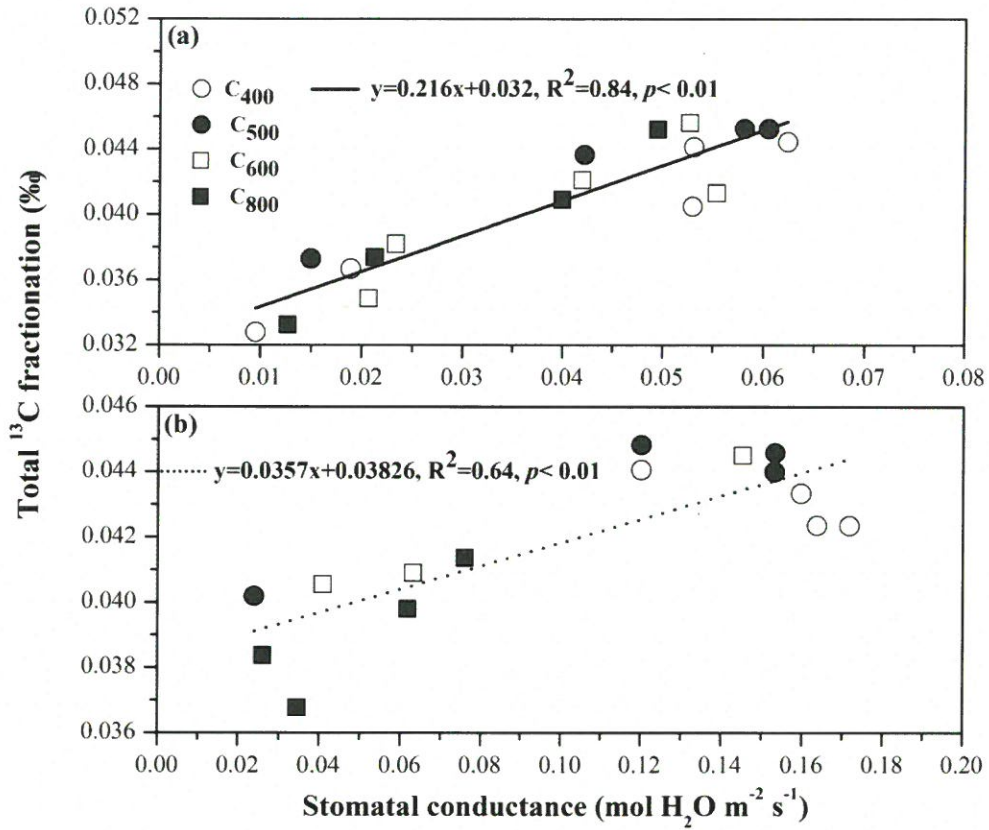
671 **Figure 4.** Instantaneous water use efficiency through gas exchange measurements ( $WUE_{ge}$ ) for leaves  
 672 from *P. orientalis* (a) and *Q. variabilis* (b) for four CO<sub>2</sub> concentrations × five soil volumetric water  
 673 content treatments. Means ± SDs, n= 32.



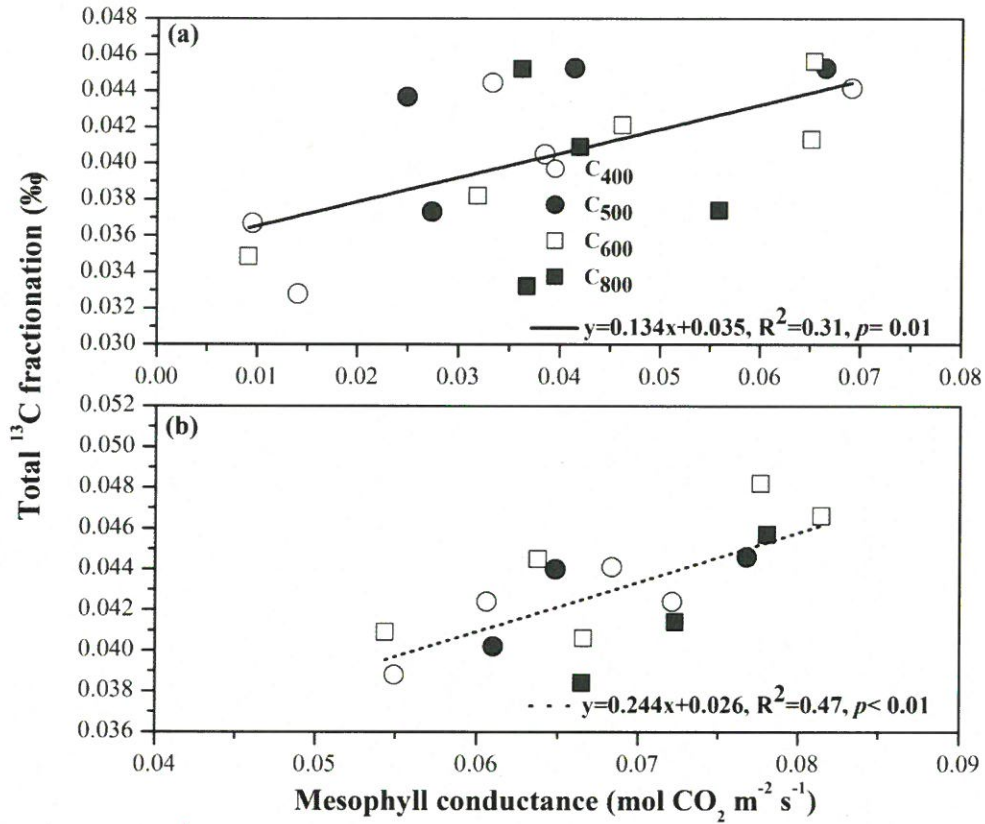
674 **Figure 5.** Instantaneous water use efficiency estimated by  $\delta^{13}\text{C}$  of water-soluble compounds (WUE<sub>cp</sub>)  
 675 from leaves of *P. orientalis* (a) and *Q. variabilis* (b) for four CO<sub>2</sub> concentrations  $\times$  five soil volumetric  
 676 water content treatments. Means  $\pm$  SDs, n= 32.



677 **Figure 6.** Mesophyll conductance in *P. orientalis* (a) and *Q. variabilis* (b) for four CO<sub>2</sub> concentrations  
 678 × five soil volumetric water content treatments. Means ± SDs, n= 32.



679 **Figure 7.** Regression between stomatal conductance and total  $^{13}\text{C}$  fractionation in *P. orientalis* (a) and  
 680 *Q. variabilis* (b) for four  $\text{CO}_2$  concentrations  $\times$  five soil volumetric water content treatments ( $p<0.01$ ,  
 681  $n=32$ ).



682 **Figure 8.** Regression between mesophyll conductance and total  $^{13}\text{C}$  fractionation in *P. orientalis* (a)  
 683 and *Q. variabilis* (b) for four  $\text{CO}_2$  concentrations  $\times$  five soil volumetric water content treatments ( $p < 0.01$ ,  $n=32$ ).



## Table

686 Table 1. Orthogonal treatments applied to *P. orientalis* and *Q. variabilis*.

<i>P. orientalis</i>	Repeats (cultivated period)	B <sub>1</sub>	B <sub>2</sub>	B <sub>3</sub>	B <sub>4</sub>	B <sub>5</sub>
A <sub>1</sub>	R <sub>1</sub> : June 2–9	A <sub>1</sub> B <sub>1</sub> R <sub>1</sub>	A <sub>1</sub> B <sub>2</sub> R <sub>1</sub>	A <sub>1</sub> B <sub>3</sub> R <sub>1</sub>	A <sub>1</sub> B <sub>4</sub> R <sub>1</sub>	A <sub>1</sub> B <sub>5</sub> R <sub>1</sub>
	R <sub>2</sub> : June 12–19	A <sub>1</sub> B <sub>1</sub> R <sub>2</sub>	A <sub>1</sub> B <sub>2</sub> R <sub>2</sub>	A <sub>1</sub> B <sub>3</sub> R <sub>2</sub>	A <sub>1</sub> B <sub>4</sub> R <sub>2</sub>	A <sub>1</sub> B <sub>5</sub> R <sub>2</sub>
A <sub>2</sub>	R <sub>1</sub> : July 11–18	A <sub>2</sub> B <sub>1</sub> R <sub>1</sub>	A <sub>2</sub> B <sub>2</sub> R <sub>1</sub>	A <sub>2</sub> B <sub>3</sub> R <sub>1</sub>	A <sub>2</sub> B <sub>4</sub> R <sub>1</sub>	A <sub>2</sub> B <sub>5</sub> R <sub>1</sub>
	R <sub>2</sub> : July 22–29	A <sub>2</sub> B <sub>1</sub> R <sub>2</sub>	A <sub>2</sub> B <sub>2</sub> R <sub>2</sub>	A <sub>2</sub> B <sub>3</sub> R <sub>2</sub>	A <sub>2</sub> B <sub>4</sub> R <sub>2</sub>	A <sub>2</sub> B <sub>5</sub> R <sub>2</sub>
A <sub>3</sub>	R <sub>1</sub> : June 2–9	A <sub>3</sub> B <sub>1</sub> R <sub>1</sub>	A <sub>3</sub> B <sub>2</sub> R <sub>1</sub>	A <sub>3</sub> B <sub>3</sub> R <sub>1</sub>	A <sub>3</sub> B <sub>4</sub> R <sub>1</sub>	A <sub>3</sub> B <sub>5</sub> R <sub>1</sub>
	R <sub>2</sub> : June 12–19	A <sub>3</sub> B <sub>1</sub> R <sub>2</sub>	A <sub>3</sub> B <sub>2</sub> R <sub>2</sub>	A <sub>3</sub> B <sub>3</sub> R <sub>2</sub>	A <sub>3</sub> B <sub>4</sub> R <sub>2</sub>	A <sub>3</sub> B <sub>5</sub> R <sub>2</sub>
A <sub>4</sub>	R <sub>1</sub> : July 11–18	A <sub>4</sub> B <sub>1</sub> R <sub>1</sub>	A <sub>4</sub> B <sub>2</sub> R <sub>1</sub>	A <sub>4</sub> B <sub>3</sub> R <sub>1</sub>	A <sub>4</sub> B <sub>4</sub> R <sub>1</sub>	A <sub>4</sub> B <sub>5</sub> R <sub>1</sub>
	R <sub>2</sub> : July 22–29	A <sub>4</sub> B <sub>1</sub> R <sub>2</sub>	A <sub>4</sub> B <sub>2</sub> R <sub>2</sub>	A <sub>4</sub> B <sub>3</sub> R <sub>2</sub>	A <sub>4</sub> B <sub>4</sub> R <sub>2</sub>	A <sub>4</sub> B <sub>5</sub> R <sub>2</sub>
<i>Q. variabilis</i>	Repeats (cultivated period)	B <sub>1</sub>	B <sub>2</sub>	B <sub>3</sub>	B <sub>4</sub>	B <sub>5</sub>
A <sub>1</sub>	P <sub>1</sub> : June 21–28	A <sub>1</sub> B <sub>1</sub> P <sub>1</sub>	A <sub>1</sub> B <sub>2</sub> P <sub>1</sub>	A <sub>1</sub> B <sub>3</sub> P <sub>1</sub>	A <sub>1</sub> B <sub>4</sub> P <sub>1</sub>	A <sub>1</sub> B <sub>5</sub> P <sub>1</sub>
	P <sub>2</sub> : July 2–9	A <sub>1</sub> B <sub>1</sub> P <sub>2</sub>	A <sub>1</sub> B <sub>2</sub> P <sub>2</sub>	A <sub>1</sub> B <sub>3</sub> P <sub>2</sub>	A <sub>1</sub> B <sub>4</sub> P <sub>2</sub>	A <sub>1</sub> B <sub>5</sub> P <sub>2</sub>
A <sub>2</sub>	P <sub>1</sub> : August 4–11	A <sub>2</sub> B <sub>1</sub> P <sub>1</sub>	A <sub>2</sub> B <sub>2</sub> P <sub>1</sub>	A <sub>2</sub> B <sub>3</sub> P <sub>1</sub>	A <sub>2</sub> B <sub>4</sub> P <sub>1</sub>	A <sub>2</sub> B <sub>5</sub> P <sub>1</sub>
	P <sub>2</sub> : August 15–22	A <sub>2</sub> B <sub>1</sub> P <sub>2</sub>	A <sub>2</sub> B <sub>2</sub> P <sub>2</sub>	A <sub>2</sub> B <sub>3</sub> P <sub>2</sub>	A <sub>2</sub> B <sub>4</sub> P <sub>2</sub>	A <sub>2</sub> B <sub>5</sub> P <sub>2</sub>
A <sub>3</sub>	P <sub>1</sub> : June 21–28	A <sub>3</sub> B <sub>1</sub> P <sub>1</sub>	A <sub>3</sub> B <sub>2</sub> P <sub>1</sub>	A <sub>3</sub> B <sub>3</sub> P <sub>1</sub>	A <sub>3</sub> B <sub>4</sub> P <sub>1</sub>	A <sub>3</sub> B <sub>5</sub> P <sub>1</sub>
	P <sub>2</sub> : July 2–9	A <sub>3</sub> B <sub>1</sub> P <sub>2</sub>	A <sub>3</sub> B <sub>2</sub> P <sub>2</sub>	A <sub>3</sub> B <sub>3</sub> P <sub>2</sub>	A <sub>3</sub> B <sub>4</sub> P <sub>2</sub>	A <sub>3</sub> B <sub>5</sub> P <sub>2</sub>
A <sub>4</sub>	P <sub>1</sub> : August 4–11	A <sub>4</sub> B <sub>1</sub> P <sub>1</sub>	A <sub>4</sub> B <sub>2</sub> P <sub>1</sub>	A <sub>4</sub> B <sub>3</sub> P <sub>1</sub>	A <sub>4</sub> B <sub>4</sub> P <sub>1</sub>	A <sub>4</sub> B <sub>5</sub> P <sub>1</sub>
	P <sub>2</sub> : August 15–22	A <sub>4</sub> B <sub>1</sub> P <sub>2</sub>	A <sub>4</sub> B <sub>2</sub> P <sub>2</sub>	A <sub>4</sub> B <sub>3</sub> P <sub>2</sub>	A <sub>4</sub> B <sub>4</sub> P <sub>2</sub>	A <sub>4</sub> B <sub>5</sub> P <sub>2</sub>

**Table 2.** Carbon-13 isotope fractionation in *P. orientalis* and *Q. variabilis* under four CO<sub>2</sub> concentrations × five soil volumetric water content treatments.

Species	SWC (of FC)	CO <sub>2</sub> concentration (ppm)											
		<sup>13</sup> C fractionation (‰)					<sup>13</sup> C fractionation (‰)						
		400	500	600	800	400	500	600	800	400	500	600	800
<i>P. orientalis</i>	35%–45%	0.0328	0.0373	0.0349	0.0332	0.0081	0.0030	0.0034	0.0072	0.0247	0.0343	0.0315	0.0260
	50%–60%	0.0367	0.0437	0.0382	0.0374	0.0018	0.0058	0.0094	0.0004	0.0349	0.0379	0.0288	0.0370
	60%–70%	0.0405	0.0366	0.0421	0.0409	0.0018	0.0050	0.0026	0.0007	0.0387	0.0316	0.0395	0.0402
	70%–80%	0.0444	0.0453	0.0413	0.0452	0.0044	0.0052	0.0103	0.0013	0.0400	0.0401	0.0310	0.0439
	100%	0.0441	0.0453	0.0456	0.0472	0.0057	0.0040	0.0025	0.0039	0.0384	0.0413	0.0431	0.0433
		Total <sup>13</sup> C fractionatio					Post- photosynthesis						
<i>Q. variabilis</i>	35%–45%	0.0388	0.0402	0.0406	0.0384	0.0007	0.0025	0.0006	0.0091	0.0381	0.0377	0.0400	0.0293
	50%–60%	0.0433	0.0448	0.0409	0.0368	0.0061	0.0084	0.0023	0.0018	0.0372	0.0364	0.0386	0.0350
	60%–70%	0.0424	0.0440	0.0445	0.0414	0.0066	0.0086	0.0078	0.0041	0.0358	0.0354	0.0367	0.0373
	70%–80%	0.0424	0.0446	0.0482	0.0457	0.0034	0.0016	0.0074	0.0028	0.0390	0.0430	0.0408	0.0429
	100%	0.0441	0.0466	0.0466	0.0398	0.0027	0.0076	0.0022	0.0125	0.0414	0.0390	0.0444	0.0273
		conductance											
		n (%)											